QUANTITATIVE COMPARISON OF 2D AND 3D MODELING FOR CONCRETE GRAVITY DAMS

A THESIS SUBMITTED TO
THE GRADUATE SCHOOL OF NATURAL AND APPLIED SCIENCES
OF
MIDDLE EAST TECHNICAL UNIVERSITY

BY
EKİN ERDEM EVLİYA

IN PARTIAL FULFILLMENT OF THE REQUIREMENTS
FOR
THE DEGREE OF MASTER OF SCIENCE
IN
CIVIL ENGINEERING

DECEMBER 2014

Approval of the thesis:

A QUANTITATIVE COMPARISON OF 2D AND 3D MODELING OF CONCRETE GRAVITY DAMS

Submitted by **EKİN ERDEM EVLİYA** in partial fulfillment of the requirements for the degree of **Master of Science in Civil Engineering Department, Middle East Technical University** by,

Prof. Dr. Gülbin Dural Ünver
Dean, Graduate School of **Natural and Applied Sciences** _____________________

Prof. Dr. Ahmet Cevdet Yalçıner
Head of Department, **Civil Engineering** _____________________

Assoc. Prof. Dr. Yalın Arıcı
Supervisor, **Civil Engineering Dept., METU** _____________________

Examining Committee Members:

Prof. Dr. Mehmet Utku
Civil Engineering Dept., METU _____________________

Assoc. Prof. Dr. Yalın Arıcı
Civil Engineering Dept., METU _____________________

Prof. Dr. Barış Binici
Civil Engineering Dept., METU _____________________

Assoc. Prof. Dr. Özgür Kurç
Civil Engineering Dept., METU _____________________

Assist. Prof. Dr. Ercan Gürses
Aerospace Engineering Dept., METU _____________________

DATE: 05.12.2014

I hereby declare that all information in this document has been obtained and presented in accordance with academic rules and ethical conduct. I also declare that, as required by these rules and conduct, I have fully cited and referenced all material and results that are not original to this work.

Name, Last name **:** Ekin Erdem Evliya

Signature :

ABSTRACT

QUANTITATIVE COMPARISON OF 2D AND 3D MODELING FOR CONCRETE GRAVITY DAMS

Evliya, Ekin Erdem
M.S., Department of Civil Engineering
Supervisor: Assoc.Prof.Dr. Yalın ARICI

December 2014, 78 Pages

Seismic behavior of gravity dams has long been evaluated and predicted using a representative 2D monolith for the dam. Formulated for the gravity dams built in wide-canyons, the assumption is nevertheless utilized extensively for almost all concrete dams due to the established procedures in 2D space as well as the expected computational costs of building a three dimensional model. A significant number of roller compacted concrete dams are being designed based on these procedures regardless of the valley dimensions, joint-spacing or joint details. Based on the premise that the assumption is overstretched for practical purposes in a variety of settings, the purpose of this study is to critically evaluate the behavior of monoliths within a dam and determine the representativeness of this assumption. A generic 80m high dam was considered in different valley settings, corresponding to multiples of the dam height. For a range of selected ground motions, the difference between the responses of individual monoliths to the full monolithic dam solution was compared in a 3D analyses setting. The results were compared to the commonly used 2D solutions. The results showed that the 2D assumption generally yielded better estimates to the 3D case for the independent monoliths and wide valleys whereas it showed large discrepancies with respect to 3D models for the fully monolithic case and narrow valleys.

Keywords: RCC, seismic design, 2D vs. 3D analyses, interface, frequency response

ÖZ

BETON AĞIRLIK BARAJLARIN 2B VE 3B
MODELLEMELERİNİN NİCELİKSEL KARŞILAŞTIRMASI

Evliya, Ekin Erdem
Yüksek Lisans, İnşaat Mühendisliği Bölümü
Tez Yöneticisi: Doç. Dr. Yalın ARICI

Aralık 2014, 78 Sayfa

Ağırlık barajlarının sismik davranışı uzun zamandır 2 boyutlu temsili bir monolit kullanılarak tahmin edilmekte ve değerlendirilmektedir. Bu varsayım geniş vadi açıklığına sahip barajlar için formüle edilmiş olmasına rağmen, 2 boyutlu uzayda kullanılan yerleşmiş prosedürler ve 3 boyutlu bir analizin zorlukları sebebiyle neredeyse tüm beton barajlar için yaygın bir şekilde kullanılmaktadır. Silindirle sıkıştırılmış beton barajların önemli bir bölümü vadi açıklığı, derz açıklığı ya da bağlantı detayı gözetmeksizin bu prosedürler ile tasarlanmaktadır. Bu varsayımın çeşitli durumlarda güvenilirliğini yitirebileceği önermesine dayanarak, bu çalışmanın amacı monolitlerin davranışını eleştirel bir şekilde değerlendirerek bu varsayımın geçerliliğini belirlemektir. Çalışmada yüksekliğin katlarına tekabül eden farklı vadi açıklıklarında, çok kullanılan bir kesite sahip 80m yüksekliğinde baraj modelleri kullanılmıştır. 3 boyutlu bir ortamda seçilen bir dizi zemin hareketinde tekil monolitlerin tepkileri, yekpare baraj çözümünün tepkisi ile karşılaştırılmıştır. Sonuçlar genelde kullanılan 2 boyutlu çözümler ile karşılaştırılmıştır. 2 boyut varsayımı bağımsız monolitler ve geniş vadiler ile ele alındığında 3 boyutlu modele daha iyi yaklaşımlar yaratırken yekpare gövdelerde ve dar vadilerde çok farklı sonuçlar verebilmektedir.

Anahtar Kelimeler: Silindirle Sıkıştırılmış Beton, sismik tasarım, 2D vs 3D analizler, ara yüzey

To all the people who have lost their lives

because of earthquakes and other natural disasters

and to those that could have been saved,

if not for the greed of others…

…

Your science will be valueless, you'll find

And learning will be sterile, if inviting

Unless you pledge your intellect to fighting

Against all enemies of all mankind…

Bertolt BRECHT

ACKNOWLEDGEMENTS

This study was carried out under the supervision of Assoc. Prof. Dr. Yalın Arıcı. I am most grateful for his help, guidance, advice, criticism, insight, and his patience throughout the course of this study.

I would like to thank my teacher Assoc. Prof. Dr. Ayşegül Askan Gündoğan for her wonderful teaching and encouragement which inspired me to follow a life of academia in the field of structural engineering.

I would especially like to thank my friends Hüsnü Yıldız, Berat Feyza Soysal and Ali Rıza Yücel for their help and contributions which were invaluable for this study.

I would also like to express my deep gratitude for all my friends who gave me much needed support throughout my studies, and my comrades with whom I share the dream of a better world and who struggle by my side for it.

My family deserves the deepest of my gratitudes. My mother Sevgi Evliya, who has always encouraged me to follow an academic carrier and has been incredibly supporting since the beginning, my father Sermet Evliya, who tought me that there are no limits to learning and has always encouraged me to outdo myself, and my sister Melodi Evliya, whom I deeply love and the support of whom, I have deeply felt every step of the way throughout my studies…

And last but not least, I must express endless gratitude and love for the woman who has been with me during both my brightest and darkest hour, who has always been at my side when I needed her and who has always managed to help me up when I stumbled… My friend, my comrade, my partner in life and crime, my love:

Cansu Tolun…

TABLE OF CONTENTS

LIST OF FIGURES

FIGURES

LIST OF TABLES

TABLES

LIST OF ABBREVATIONS

2D	:	Two-Dimensional
3D	:	Three-Dimensional
c	:	Cohesion (Coulomb Friction Model)
E	:	Young's Modulus
E_c	:	Young's Modulus of Concrete
E_f	:	Young's Modulus of Foundation
FFT	:	Fast Fourier Transform
FN	:	Fault-Normal
FP	:	Fault-Parallel
IDA	:	Incremental Dynamic Analysis
MCE	:	Maximum Credible Earthquake
MF	:	Massless Foundation
MSE	:	Mean Square Error
OBE	:	Operation Basis Earthquake
PGA	:	Peak Ground Acceleration
PGV	:	Peak Ground Velocity
PSA	:	Pseudo-Spectral Acceleration
RCC	:	Roller Compacted Concrete
R_{jb}	:	Joyner-Boore Distance
R_{rup}	:	Rupture Distance
SDOF	:	Single Degree of Freedom
SSI	:	Soil-Structure Interaction
T	:	Period
V/H	:	Valley Width to Dam Height Ratio
V_{s30}	:	Time averaged shear wave velocity over the top 30 meters of the underlying soil

CHAPTER 1

INTRODUCTION

1.1. GENERAL

The use of roller compacted concrete for the construction of gravity dams are popular for the hydroelectric power generation in the emerging economies. Majority of the old dam stock in the developed world are also gravity dams built using conventional concrete. Given the need for the design of new systems in the developing world, along with the need for the evaluation of the seismic performance of the old stock in the developed countries, analysis technique for the gravity dam structures becomes an important issue for the designers, owners and the regulators. This is due to the fact that soil-structure interaction, which is usually not considered in the design process for conventional infrastructure, is important in defining the performance of such systems. The presence of soil-structure interaction significantly affects the response of these structures and the consideration of the effect often leads to a reduction in the predicted response quantities.

The analyses of these systems are usually conducted with a two dimensional (2D) modeling approach, using a frequency domain linear or time domain nonlinear analyses. Given the many different properties regarding the topography, material, foundation etc., the prevalence of 2D analyses for dam systems is somewhat peculiar. This approach stems from the historical development of the analysis methods for these systems as well as the traditional construction technique of these systems as independent monoliths separated by construction joints. However, with the extensive use of the RCC material, construction joints are formed usually by rotary saws in RCC dams. Partial slicing at the upstream or downstream façades, zipper-style connection details varying the location of the joint for each lift and significantly extending the joint spacing are among the employed variations to the old construction techniques. Gravity dams were also treated as 2D structures based on the wide valleys they were built in, as arch dams were typically designed in narrow valleys. With the significant speed advantage provided by RCC construction, gravity dams are now built even in narrow valleys otherwise suitable for arch dams.

In spite of the factors presented above, engineers hardly think about the possible three dimensional (3D) effects of the seismic loading on such systems 1) 3D model preparation, analysis and post processing is time consuming 2) based on precedence as historical norms and experience dictating 2D analyses, 3) as they do not possess the tools, 4) as they assume conventional joint behavior and 5) consider the arching effect as the only important 3D effect. The goal of this thesis is investigating the accuracy of the conventional analysis techniques based on these premises. A short review on the literature on the subject and the specific goals and the limitations of the study are given in the next sections.

1.2. LITERATURE REVIEW

Pioneering studies on the seismic analysis of concrete gravity dams were conducted by Westergaard [1], who developed the technique of modeling the hydrodynamic effects of a reservoir using added masses on the upstream face of the dam using 2D modeling. This technique ignored the effects of water compressibility. The response of concrete gravity dams including the effect of reservoir-dam body interaction and the effect of water compressibility and the earthquake resistant design of concrete gravity dams considering these effects were investigated by Chopra [2,3] using 2D modeling. The effects of hydrodynamic interaction and water compressibility were later investigated using 3D modeling for arch dams by Hall and Chopra [4] in 1980. They have concluded that the inclusion of water compressibility significantly influence the seismic response of concrete gravity dams. The response of the system becomes dependent on the reservoir shape with the inclusion of water compressibility.

Earthquake response of concrete gravity dams was investigated including the dam-foundation interaction and a simplified analysis technique, in which the response of the fundamental vibration mode of the system is modeled as a single degree of freedom system underlain by an elastic half-space foundation, was developed by Fenves and Chopra [5-7]. A finite element technique for obtaining a 2D rigorous solution of dam-water-foundation systems which includes both the reservoir-foundation interaction and a layered foundation was developed by Lotfi et al. [8]. The effect of sedimentation on the overall behavior of the dam-foundation-reservoir system was investigated including a layered foundation using boundary element technique in a 2D setting by Medina et al. [9] and later using finite element technique by Bougacha and Tassoulas [10].

Studies on the non-linear response of concrete gravity dams started in the last two decades given the frequency domain formulation requires a linear system formulation. Earthquake induced base sliding of concrete gravity dams was investigated by Chopra and Zhang [11] and the overall response including the base sliding effect was investigated by Chávez and Fenves [12] using a hybrid time-frequency formulation. Studies including non-linear effects of cracking behavior of concrete were conducted by Bhattacharjee and Leger [13] and later by Leger and Leclerc [14] using a smeared crack model to determine the propagation of cracking on the system. The literature presented above provides investigations on the complex problem of accurately modeling reservoir-dam-foundation systems. Dam-reservoir-foundation interaction and non-linear response due to cracking and joint behavior are the two main phenomena which define the response of these systems. There is a lack of studies that take these two main problems in dam engineering into consideration simultaneously. Since the focus of this study is on the comparison of 2D and 3D modeling for concrete gravity dams, soil-structure interaction was the main consideration in modeling these structures.

SSI effects have an important role in determining the overall dynamic behavior of large infrastructure systems. This issue has been recognized for nuclear structures somewhat earlier than dams in which the major issue was the simulation of non-reflecting boundary conditions for a seismic problem. Most of the studies on this field, developed separately and parallel to the literature on dam systems, have focused on the issue of correctly defining the boundary conditions of the system to correctly simulate this behavior, such as the work of Lysmer and Kuhlemeyer [15] which led to the development of the software SASSI (System for Analysis of Soil Structure Interaction) by Lysmer et al. [16]. A more detailed literature review in this area is not provided here with the scope of the thesis limited to dam systems.

The most prominent works on the effect of SSI on concrete dams are perhaps the studies mentioned above by Fenves and Chopra [5, 6] and Medina et al. [9]. These studies are concerned with the response of the dam systems conducted in the frequency domain, thus limiting the results in the linear-elastic range. Provisions for design and evaluation of concrete gravity dams [17, 18] based on the SDOF solution in [6] is widely used for design and evaluation purposes providing a technical background for the use of the Finite Element Method considering equivalent SSI effects.

The studies by Fenves and Chopra [5, 6], predominantly effective in shaping the practice in the field is based on the following assumptions:

- Concrete gravity dams are modeled in a 2D frequency domain analysis. [5] The contribution of the first vibration mode is dominant in the overall response of the system. In this sense it is a valid assumption to simplify these systems as SDOF systems with equivalent damping ratios [6].
- Complex natural vibration modes are neglected by assuming a rigid contact surface behavior between the dam body and the foundation.
- In order to utilize a frequency domain solution, the soil medium beneath the dam body is idealized as a linear-elastic half-space in order to obtain a semi analytical solution. [5]

The assumptions presented above present the following disadvantages:

- This method [6] suggests the use of an equivalent damping ratio for gravity dam systems. However, it is only valid if the contribution of the first vibration frequency is dominant in the overall behavior. Since any changes or irregularities in the dam type and geometry affect the contribution of the first fundamental mode, the method should be used cautiously for dams with different geometries.
- Since the soil beneath the dam is considered as an infinite medium, soil properties beneath the dam superstructure are assumed to be constant and/or

there is no stiff rock in a considerable depth. A significant number of dams are built on layered soils and/or stiff rock formations which renders this assumption unrealistic.

- The frequency based solutions do not permit any non-linear solutions for both the dam and the foundation.

The latter of the methods presented above, presented by Medina et al. [9] utilizes a layered medium for the foundation using Boundary Element Method. This approach considers the dam as a triangular shaped structure on layered strata underlain by stiff rock. The structure is considered as a multi degree of freedom system, thus taking into account all vibration modes, and contact behavior is defined as flexible. However due to the ease of computation of the SDOF solution in the former solution, the former method is widely used for simplicity instead of the Boundary Element Method solutions.

Perhaps the major disadvantage for both methods is the requirement to employ a frequency domain solution which limits the response to linear behavior. Since the behavior of the dam is expected to be non-linear to some extent (interface behavior, cracking, etc.) a time domain non-linear solution considering both the plasticity effects and SSI is required. Given such tools require very costly computations not readily available to practicing engineers, models with massless foundations remain as important alternatives to represent SSI effect and nonlinearity together in the design process.

With the widespread use of finite element modeling and other computational techniques, several software were developed for the analysis of dams. One of the pioneering works in this field was the software ADAP (Arch Dam Analysis Program) developed by Clough et al. [19]. ADAP, which was generated from the software SAP, was capable of conducting 3D analyses of arch dams. Later, the platforms EAGD and EACD were developed over the course of time for the earthquake analysis of concrete gravity dams in 2D and 3D settings, respectively, by Chopra and his colleagues. [20-23] Reservoir-structure-soil interaction is considered rigorously in these platforms. A uniform canyon extending to infinity is one of the major limiting assumptions for the code EACD which was developed for the seismic analyses of arch dams. As mentioned above, due to the frequency domain limitation, these platforms do not permit any non-linear approach to the problem.

As given above, the three dimensional approach to the problem was developed in the context of arch dams by using three dimensional finite and boundary element methods. A study using boundary element method for modeling arch dam systems in 3D space including the dam-reservoir-foundation interaction was conducted by Dominguez and Maeso [24]. Full reservoir condition including water compressibility and a linear viscoelastic foundation was assumed in this study. Effects of sedimentation on large structures subject to fluid-soil-structure interaction including arch dams were investigated in 3D space by Aznárez et al. [25]. Non-linear behavior due to earthquake induced cracking in concrete was investigated for arch dams using the discrete and non-orthogonal smeared crack method and a finite element program utilizing a combination of these two methods was developed by Lotfi and Espandar [26]. As given above, gravity dams are hardly considered to be in the scope of the 3D analysis tools. A single monolith including the reservoir was modeled in 3D by Arabshahi and Lotfi [27] in order to investigate the effect of the non-linearity in the dam-foundation interface on the monolith behavior. A full-scale model was not considered in this study.

The major part of the literature on the seismic analysis of dams includes the assumption of a representative 2D behavior of a monolith governing the design of the dam system. The academic world, led by the challenge provided by the SSI problem, led the practitioners to extensively use the outcomes of these studies in a 2D setting, regardless of the basic assumptions enabling the use of a 2D model, i.e. 1) A plane stress condition permitted by the use of intermittent expansion joints separating monoliths or 2) A plane strain condition for a system constructed in a wide valley. Almost all of the RCC dams built in Turkey in the last decade do not satisfy these conditions. The effect of the contraction joint behavior was only treated in the context of arch dams [26]. In their study focused on the hydrodynamic effects on a short length dam, supported by past experience, Rashed and Iwan [28] pointed out that while the 2D assumption would be satisfactory for dams with large valley width to height ratios, 3D analyses would be required for dams in narrow canyons. Despite this early evaluation, three dimensional analyses were rarely employed in the design of concrete gravity dams, but only been used for RCC dams remarkably lacking any expansion joints [29-30]. The significant difference between the 2D and 3D predictions were shown in these studies.

In light of the literature presented above, a study on the comparison of 2D and 3D modeling for concrete gravity dams was required due to the deficiency of the 3D consideration of the problem in the literature despite the expressed need for this approach and the need for a critical evaluation of 2D modeling for concrete gravity dams.

1.3. OBJECTIVE AND SCOPE

In the context of the discussion above, the main purpose of this study is to:

- Investigate the validity of the 2D single monolith approach for concrete gravity dams by comparing its response to that of its 3D counterparts.
- Investigate the effects of construction joints which is absent in the much used 2D modeling approach.

For this purpose, the investigation of 2D and 3D modeling for concrete gravity dams was carried out under two main headings; the comparison of the idealized 2D and 3D responses for the system and the effect of construction joints on the response, as outlined below:

- The comparison of the idealized 2D and 3D Response.
    - Comparison of the frequency response functions of 2D and 3D models
    - Comparison of the fundamental frequencies of the 2D and 3D models
    - Comparison of the effective damping of 2D and 3D models
    - Comparison of time domain demand parameters by using transient analysis results with a suite of ground motions
- Investigation of the effects of joint properties on the system performance
    - The effect of interface material properties and non-linear behavior induced by a friction-slip model

- The effect of the opening and closing of the joints between the monoliths
- The effect of ground motion variability and directionality by utilizing bi-direction ground motions

Chapters 2 and 3 describe the numerical models used and the analysis techniques employed throughout the study.

In Chapter 4 the frequency response functions of two types of idealized 3D models are compared with idealized 2D models. The first 3D model employed was a monolithic dam system while the second model was comprised of independent monoliths. In order to account for the effects of the valley geometry, a range of valley widths ranging from one quarter to ten times the dam height were used. The results obtained from the analyses conducted with these models were compared to those of a 2D model employing the massless foundation approach as well as the theoretically robust 2D frequency domain solution considering the structure-foundation interaction. This comparison was conducted for a range of different foundation to structure stiffness ratios. Given the need for the comparison of engineering response parameters in time domain, a set of 70 motions were then used to compare the peak time history response values between 2D and 3D models.

The effect of the monolith interface response on the dam behavior is investigated in Chapter 5. In the first part of the chapter, the underlying assumptions for the independent monolith behavior were investigated. A set of analyses using the same ground motion record with different scale factors was conducted on models with different interface properties in order to determine the effect of interface properties on the chosen demand parameters for different ground motion intensities. These results were also compared with those obtained from the 2D solution. The effect of ground motion variability on the interface behavior was investigated for different valley widths using ground motion pairs scaled to fit a target spectrum. Two horizontal components of the motion were used separately in these analyses in order to investigate the motion of the dam monoliths parallel and perpendicular to the cross-stream direction. In the second part of Chapter 5, the required joint opening for the independent behavior of a gravity dam monolith was investigated conducting a number of time history analyses with 35 different ground motion pairs.

A brief summary and the overall conclusions of the study and possible avenues of future research are presented in the last chapter.

1.4. ASSUMPTIONS AND LIMITATIONS

The study is subject to the following assumptions and the limitations they impose.

- In the first part of the study, the reservoir-dam body interaction was not considered (empty reservoir was assumed) within the study in order to limit the scope of the problem. The hydrodynamic effects and the water compressibility will affect the behavior of the overall system for a full reservoir condition.
- In the second part of the study a full reservoir case was investigated using the added mass method proposed by Westergaard [1] thus the compressibility of water was not taken into account. Hall and Chopra [4] state that the effect of water compressibility is significant in the response of concrete gravity dams. According to Chopra [31] neglecting water compressibility will affect the behavior of dam systems that have a higher structural stiffness. (Stiffness range of the concrete used in real systems are considered to be in this range) However the values of demand parameters obtained in this study are used for purposes of comparison with their counterparts obtained from different models. Therefore the absolute values of these demand parameters are less significant than the relative difference between them.
- Given the primary purpose of the study for comparing the 2D/3D behavior, the dam and foundation models used in the analyses were assumed as linear elastic. Nonlinearity was only considered for the interface behavior when necessary in order to represent the joint opening/closing or sliding behavior.
- The spatial asynchronous nature of the ground motion was not considered in the analyses.

- Massless foundation approach was employed for all of the 3D models and for some of the 2D models in order to model the non-reflecting boundary for soil-structure interaction. (i.e only the flexibility of the foundation is taken into account along with stiffness proportional damping) Equivalent damping coefficients were used which were calculated in accordance with [18]. According to Chopra [31] this assumption leads to overestimation of demand parameters when compared with the solutions obtained by including all effects of dam-foundation interaction and the degree of overestimation increases as the E_f/E_c ratio decreases. (i.e as the foundation gets softer.) However, this assumption still remains an important tool for designers to combine the SSI effects with nonlinearity on the dam body for response prediction.
- Lower order elements were used in the finite element models for ease of computation with the large models which might affect the accuracy of the results.

CHAPTER 2

NUMERICAL MODELING OF 2D AND 3D RESPONSE

2.1. FINITE ELEMENT MODELS

Numerical modeling of dam behavior is often evaluated using finite element modeling technique. The finite element models in this study were built and analyzed in the software Diana. (TNO DIANA) Two different types of 3D finite element models were used in order to assess the behavior of dam systems (Figure 2.1). The first type of model was fully monolithic, representing RCC dams built with interlocking expansion joints and/or partial expansion joints. The second type represents the typical gravity dam construction, (applicable to some RCC dams with fully sawed expansion joints), with independent monoliths connected by surface interface elements. This modeling is convenient since a friction joint representing grouted or calcified joint system within an interlocked monolith system can be obtained using a typical Coulomb friction model at the interface. For the sake of simplicity, all the systems considered within the study were assumed as 80m high with the cross-section geometry shown in Figure 2.2. A 45 degree grade was assumed for the 3D models on both of the valley ends. Massless foundation models are extensively used for the prediction of non-linear behavior of the system. Given the extensive use of these models, [24, 28, 30, 31] this modeling technique was considered for 3D modeling. The abbreviation MF is used from now on to represent the massless modeling when required.

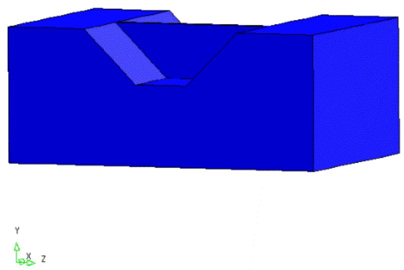

(a) Monolithic Model

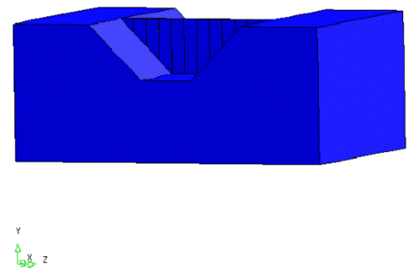

(b) Independent Monoliths

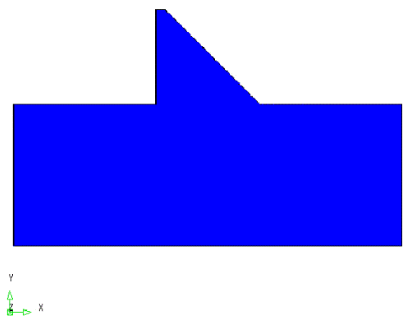

(c) 2D Model

Figure 2.1 - Finite Element Models

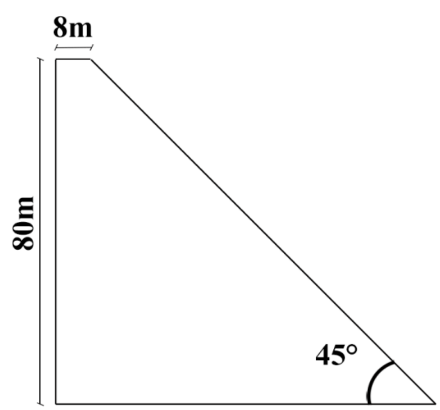

Figure 2.2 - Cross Section of the Dam

For 3D models, the width of the valley was chosen in multiples of the dam height. Five different valley widths were considered throughout the study ranging from one quarter to ten times the dam height. Models with valley widths of 0.25H, 1H, 2H, 4H, and 10H are denoted as 0x, 1x, 2x, 3x,4x, and 10x respectively. It should be noted that these values represent the width of the valley base in the center. (i.e the width at the sides is not included.) Due to the 45 degree grade, the width of each side of all models is equal to the dam height. For example the model denoted as 1x has a valley width of 80m (1H) in the center and 80m on each side totaling to 240m valley width. Furthermore the models are given a suffix "i" or "m", denoting whether the system consists of independent monoliths or is a fully monolithic system respectively. For example the model with 240m valley width and independent monoliths is denoted as "1xi". The respective valley widths of each model can be found in Table 2.1. The cross section dimensions and the visual representations of these models can be found in Figure 2.3.

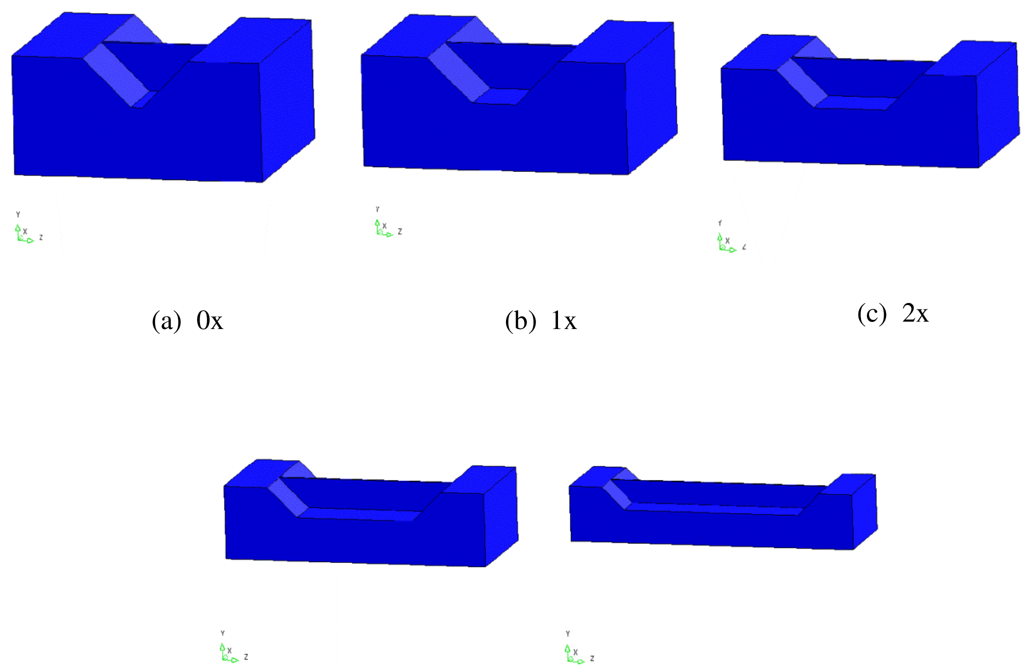

(a) 0x (b) 1x (c) 2x

(d) 4x (e) 10x

Figure 2.3 - 3D Models With Different Valley Widths

Four-node, three-side isoparametric solid pyramid elements (tetrahedron) (denoted as TE12L in the Diana software) were used in modeling both the dam body and the underlying foundation. (Figure 2.4) Lower order elements were used for the ease of computation with very large models employed in the study. The elastic properties assumed for the dam body are as follows:

Young's Modulus, E=20 GPa

Poisson's Ratio, ν=0.20

Unit Weight, ρ=2400 N/m^3

The width of the valley, the size of the monoliths and the foundation modulus were treated as the variables effective in determining the response of the system in the first section of the study, while the interface properties were treated as the determining parameters in the second part of the work. While the Young’s modulus of the foundation varies between different models, (ranging from 0.5 times to 4 times the modulus of the dam body) Poisson’s Ratio, ν, was assumed as 0.25 in all models.

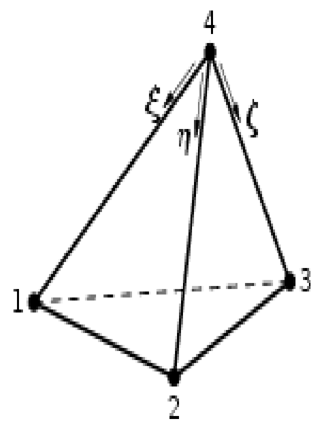

(a) Dam Body / Foundation Elements

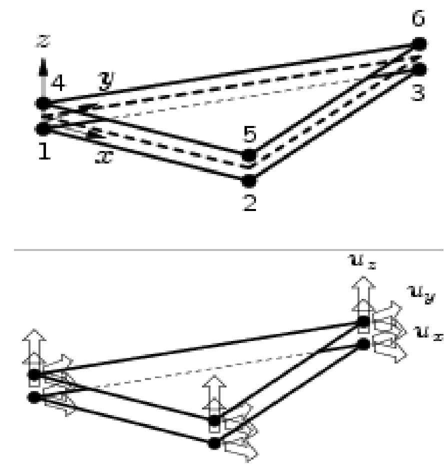

(b) Interface Elements

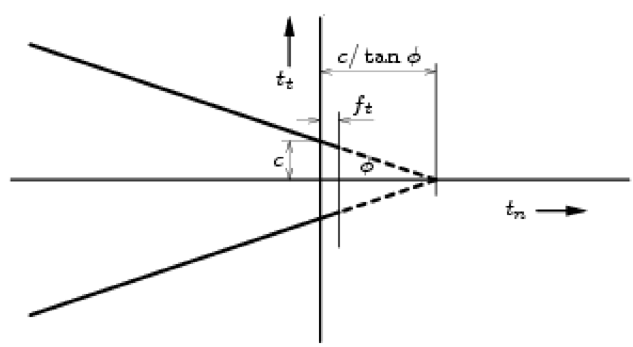

(c) Constitutive Model

Figure 2.4 - Structural Elements Used in the 3D Models
(c: Cohesion, φ: Friction angle, f_t: Tensile Strength)

Table 2.1 - Valley Widths of 3D Models

Model Name	Valley Width (Including Sides)
0x	180 m
1x	240 m
2x	320 m
4x	480 m
10x	960 m

Given the precedence of 2D analyses in the practice, two 2D solution methods were considered in this study. First of which is the plane stress model, with a massless foundation assumption, typically used in the nonlinear analyses of such systems in the time domain. Three types of elements were used in this model. For the modeling of the dam body, eight-node quadrilateral isoparametric plane stress elements (denoted as CQ16M in the Diana Software) were used. For the modeling of the foundation, six-node triangular isoparametric plane stress elements (denoted as CT12M in the Diana software) were used. Three-by-three node two dimensional interface elements (denoted as CL12I in the Diana software) were used for modeling the interface between the dam monoliths. The elements used in the modeling of 2D FEM model can be found in Figure 2.5.

The second 2D solution method employed was the theoretically robust solution of the 2D dam-foundation interaction problem in the frequency domain. [6] This solution also forms an important part of the literature as the equivalent damping on time domain models was obtained from single mode simplification of the analysis results in order to emulate this approach. [8] Accordingly, the damping ratios for the time domain models were assumed based on this methodology, i.e. the additional damping brought in by the soil-structure interaction was represented by Rayleigh damping coefficients in time domain models.

The visual representations of three types of FE models (3D Monolithic, 3D Independent and 2D) used in the study can be found in Figure 2.1.

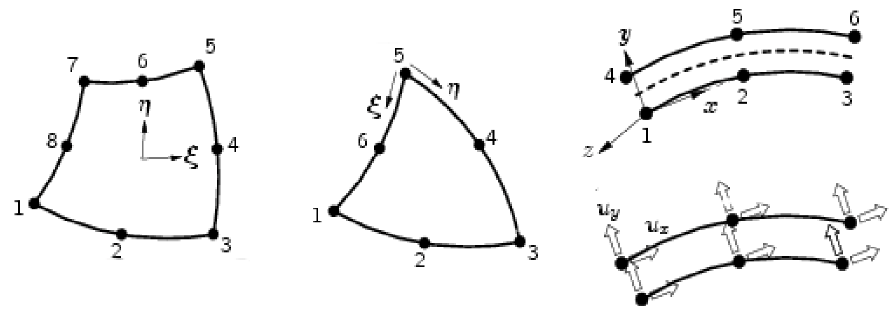

(a) Dam Body Elements (b) Foundation Elements (c) Interface Elements

Figure 2.5 - Structural Elements Used in 2D Model

2.2. THE MODELING OF THE CONSTRUCTION JOINTS

The boundaries and interface elements in the 3D models (such as those between the monoliths of the dam) were modelled using three-node triangular interface elements based on linear interpolation. Each construction joint was modeled with a range of such elements as given in Figure 2.4. As well as the advantage of being able to model completely independent monoliths using very low linear elastic stiffness at the interface elements, these models can also be used to represent the opening/closing or sliding/locking behavior between the monoliths.

The Coulomb friction model was used to simulate the stick-slip behavior at the interfaces of the monoliths. The displacement at an interface Δu is decomposed into an elastic, Δu^e and plastic part, Δu^p. (i.e., $\Delta u = \Delta u^e + \Delta u^p$) The Coulomb friction model employs the following yield (f_I) and plastic potential (g_I) surfaces defined in terms of the normal traction t_n and the tangential traction t_t .

$$f_I = \sqrt{{t_t}^2} + t_n tan\phi_I - c_I = 0 \quad \textbf{(1)}$$

$$g_I = \sqrt{{t_t}^2} + t_n tan\vartheta_I \quad \textbf{(2)}$$

Where $\tan\phi_I$ and c_I are the friction coefficient (tangent of friction angle) and the cohesion, respectively. $Tan\vartheta_I$ represents the tangent of the angle of dilatancy. The rate of plastic displacement $\Delta\dot{u}^p$ is governed by:

$$\Delta\dot{u}^p = \dot{\lambda}\frac{\partial g}{\partial t} \quad \textbf{(3)}$$

where $\dot{\lambda}$ is a multiplier. The tangent stiffness matrix is nonsymmetrical if the friction angle is not equal to the dilatancy angle ($\phi_I \neq \vartheta_I$).The interfaces in the model are mostly characterized by the transverse and normal stiffness, cohesion and the friction angle of the material used. For modeling the interfaces possible variations in these parameters were considered in accordance with the nature of the expansion joint or the construction details.

The monolithic 3D model represents the case for which the expansion joints offer full resistance to lateral movement. The independent monolith model in 3D setting represents the ideal case in which the monoliths can move independently from each other with little shear resistance. In essence, the behavior of a system was expected to be in between these idealized models governed by the nonlinear slip behavior between the monoliths.

CHAPTER 3

ANALYSIS METHODOLOGY

3.1. EIGEN ANALYSIS AND RESPONSE BOUNDS

Eigenvalue analysis is a valuable and simple tool to evaluate the dynamic behavior of a dam system as the different interaction modes between the monoliths can perhaps best be compared by the simple visualization of the mode shapes. Such a sample analysis was conducted for a generic dam located in a narrow valley of 240m width. The first three natural modes of the system are presented in Figure 3.1 for the idealized fully monolithic and independent monolith cases and the representative 2D model. As can be seen from the first fundamental frequencies in Appendix A, the monolithic system was significantly stiffer compared to the system comprised of independent monoliths that can act independently along and perpendicular to the dam axis. However, the 2D model appeared to be the most flexible among these models with a substantially reduced fundamental frequency value. Naturally, the 2D model could not predict the deformation in higher order 3D modes: in plane deformation of the monolith was observed for the higher modes of this model.

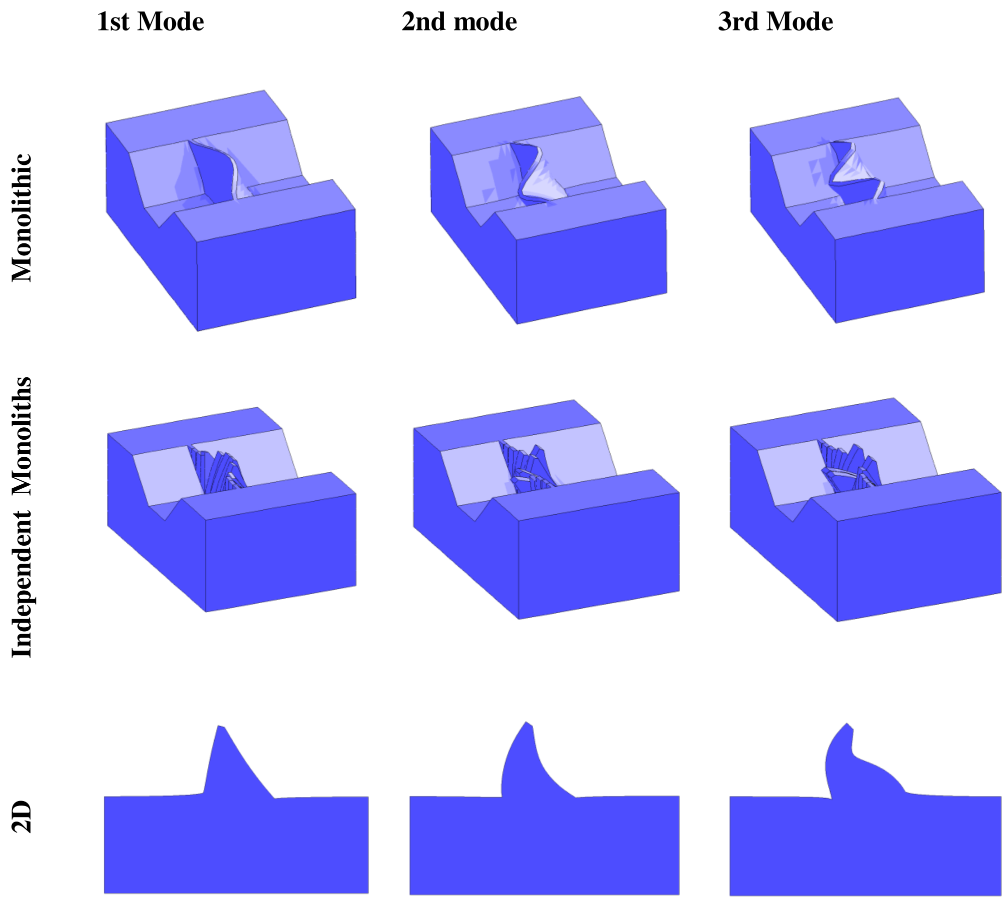

Figure 3.1 - Eigen Modes for the Model 1x and the 2D Model

The 2D modeling of gravity dam systems is significantly common in contrast to the results provided in Figure 3.1. Although the question of 2D vs 3D modeling is very commonly voiced in theoretical discussions or in an academic setting, 2D modeling is almost always preferred in the industry except for the design and evaluation of arch dams.

3.2. FREQUENCY RESPONSE OF DAM SYSTEMS

Soil-structure interaction is the primary factor determining the seismic behavior of concrete dams. Given the prevalence of this issue on the problem, as well as the requirement of a frequency domain solution, frequency response functions have been used as the common tool for assessment purposes in determining the behavior of dams while using the robust analyses techniques. In order to compare the behavior of 3D models (comprised of monolithic dam and independent monoliths) to 2D models, a simple analysis methodology to obtain frequency domain functions were utilized here. Given the full frequency response matrix is hard to obtain and even harder to present, the frequency response function for the crest acceleration at the center of the dam system was used as the representative tool. The frequency response function for the systems utilized were obtained applying a pulse with a very short duration as the base excitation of the system. Time history analyses with the pulse as the input motion were conducted for each model. The output, which was the time history of the crest acceleration at the center of the dam, of each analysis, was then converted into frequency domain by applying a Fast Fourier Transform (FFT). The transfer functions of the models were obtained by dividing the FFT of the output by the FFT of the base excitation, which was the pulse. An example of the procedure is shown in Figure 3.2 for a single model.

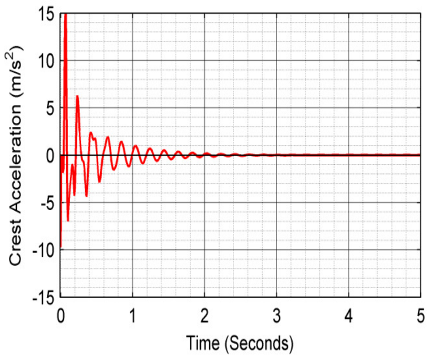

(a) Time History of Output Crest Acceleration obtained from time history analysis with a pulse as the input motion.

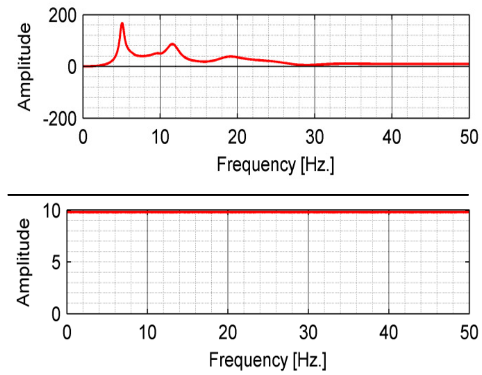

(b) Absolute value of FFT of output and input. Output is divided by input to obtain Transfer Function

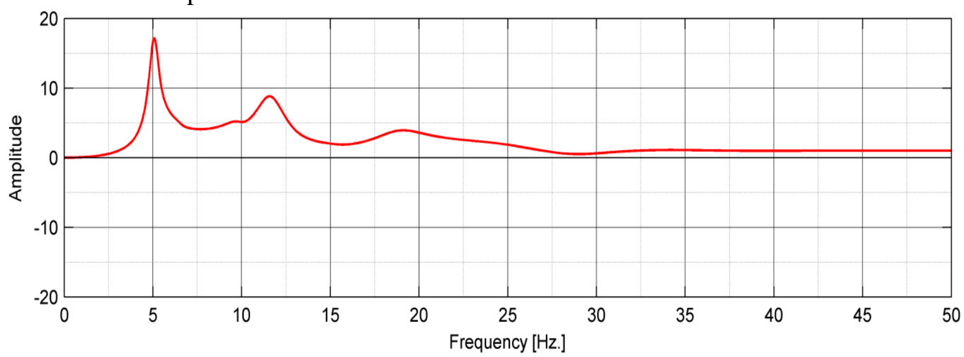

(c) Single Input-Single Output Transfer Function

Figure 3.2 - Procedure For Obtaining the Frequency Response Function

While the frequency response function is an effective tool for evaluating the effectiveness of the analytical models, it can hardly be used within an evaluation or design process. It is very hard to compare the results of two analysis models in a quantitative sense, as qualitative evaluation is the only means to compare a set of results from such models. Moreover, solutions to an engineering problem are usually based on time domain quantities, such as stresses, strains or displacements, which can formally be introduced as limiting or target quantities. The frequency response function offers a very rapid method of obtaining the output response for any given input. Sidelining the time consuming formal step wise integration method in the time domain (corresponding to the convolution integral), one can obtain the output time history response by multiplying the frequency response function by the FFT of the input motion. An example is shown in Figure 3.2. The aforementioned procedure provides a tool to compare the different frequency functions for different input motions in the domain by comparing peak response quantities.

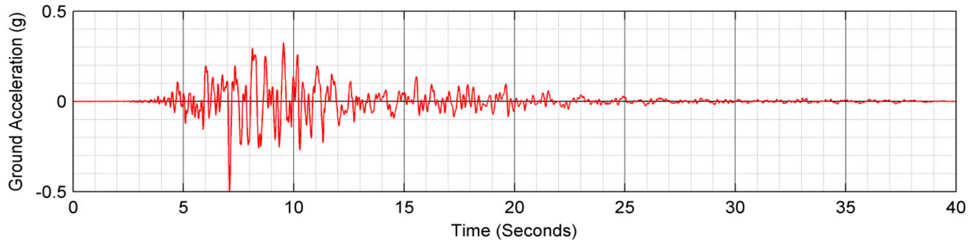

(a) Time History of Input Ground Motion

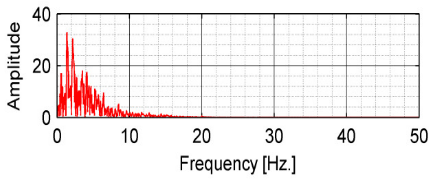

(b) Fourier Transform of the Input Motion

x

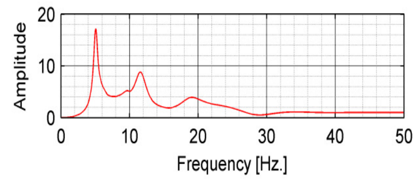

(c) Transfer Function of the Model

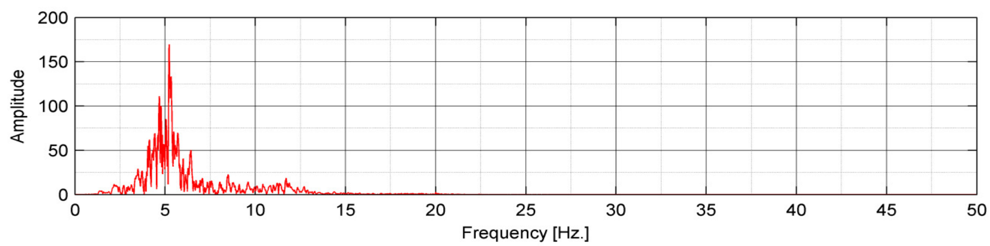

(d) Response of the system (crest acceleration in the center) to the input motion in frequency domain

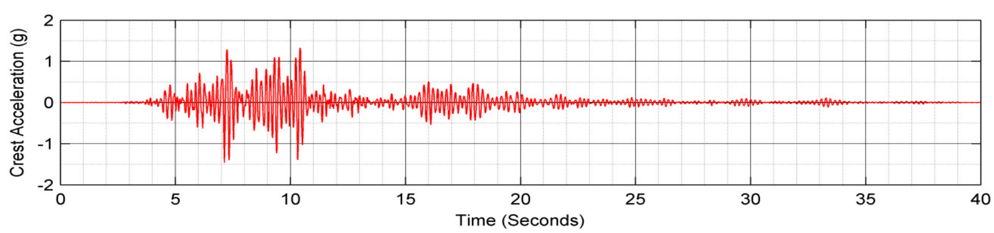

(e) Response of the system in time domain obtained by the Reverse Fourier Transform of the above spectrum

Figure 3.3 – Procedure for Applying a Ground Motion Using the Transfer Function

3.3. MESH CONVERGENCE

In order to determine the adequacy of the mesh density used in the 3D models, a mesh convergence investigation was conducted on the model 1x (Valley Width=240m) which is the model most frequently used throughout the thesis. The frequency response functions of three different models with different mesh densities in addition to that of the original model were compared. These models were built such that the geometry of the dam remained the same while the mesh density increased. The number of nodes in each model, denoted as M1, M2, M3, M4 (M1 being the original model which was used throughout the thesis.), are 2412, 6616, 14710 and 25855 respectively.

The frequency response function of each model with E_f/E_c=0.5 was calculated in the fashion described in the previous sections and presented in Figure 3.4. It can be seen in the figure that there is almost no difference in amplitude of the first vibration mode between the frequency response of M1 and M4 where the latter has more than 10 times the number of nodes of the former. There is a slight shift in the natural frequency which corresponds to a change of 8.4% in the first vibration frequency. Significant increases in the density of the mesh leads to no significant changes in both the amplitude and the fundamental frequency in the frequency response function. There is however a marked discrepancy in the second mode regarding both the amplitude and the frequency. The Fourier Spectra of the ground motion records used in this study are presented in Figure 3.5. It can be seen in this figure that for frequencies larger than 6 Hz, the amplitude is significantly reduced with respect to smaller frequencies. Therefore the discrepancy in the second vibration mode is not likely to have a significant effect on the transient analyses conducted using these ground motion records.

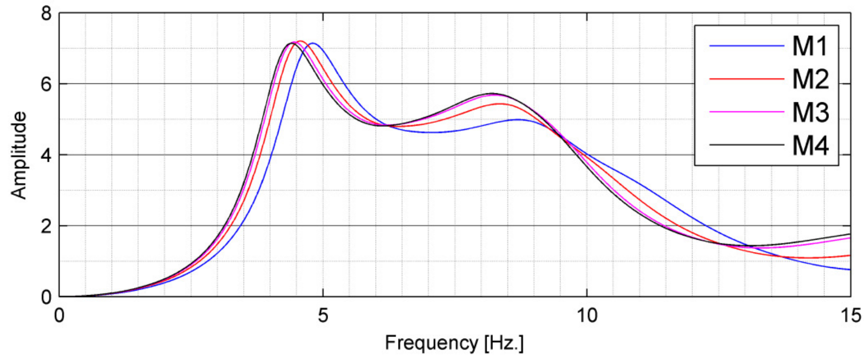

Figure 3.4 – Frequency Response Functions for Different Mesh Densities

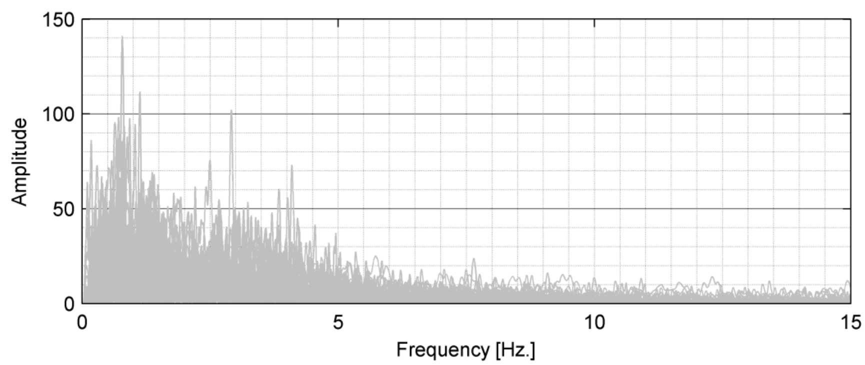

Figure 3.5 – Fourier Spectra of Selected Ground Motions

In addition to the frequency response functions, time domain demand parameters (mainly stress) were also utilized in this study. Therefore a comparison of stress results for a single input ground motion for different mesh densities was also carried out. As it will be later used in Chapter 5, a single ground motion was applied to the models and the maximum principal tensile stress values were obtained from the toe. The maximum principal tensile stress obtained from the toe area of each model are 1.19 MPa, 1.74 MPa, 1.83 MPa and 2.24 MPa for M1,M2,M3 and M4 respectively. There is an evident discrepancy in the stress results between models with different mesh densities as expected. Models with finer meshing are expected to present larger stress results. In order to compare the consistency of the models in terms of stress values, a different approach to comparing the stress results was utilized. A single element in the coarsest mesh (M1) was selected. Then, the mean of principal tensile stress histories of all the elements, which have a centroid residing inside the coordinates of the selected element volume in M1, was obtained for M2, M3 and M4. The stress time histories obained from this comparison is presented in Figure 3.6. It can be seen from this figure that the discrepancy in the stress results decreased when the mean value within the same volume is considered. Therefore it was concluded the mesh density of M1 is determined to be adequate for the purposes of this thesis.

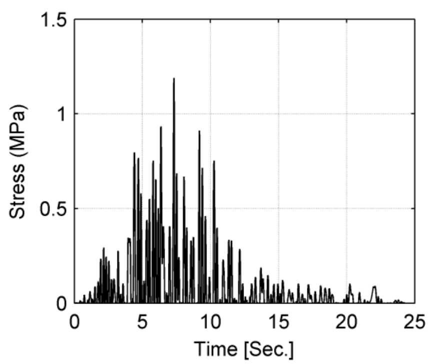

(a) M1

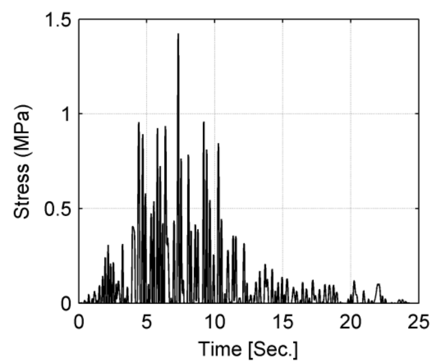

(b) M2

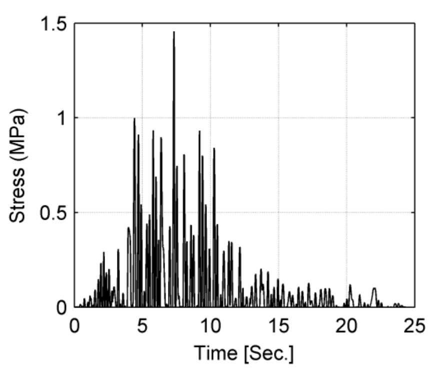

(c) M3

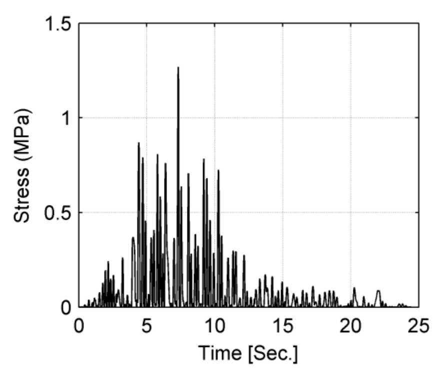

(d) M4

Figure 3.6 – Stress Time Histories for Different Mesh Densities

3.4. TRANSIENT ANALYSES OF DAM SYSTEMS

Transient analyses of the dam systems were conducted in both the time and frequency domain in this study. Time domain transient analyses were conducted using Newmark integration in the general purpose finite element program DIANA. Average acceleration method was used along with varying time steps (depending on the input ground motion) and Rayleigh damping. Rayleigh damping coefficients were computed in the customary fashion in accordance with Appendix D of USACE [18] to account for the effect of a massless foundation, an effective damping ratio was calculated for each model depending on;

a) Stiffness ratio of the foundation and the dam body: E_f/E_c

b) First natural vibration period of the structure: T_1

c) First natural vibration period of the structure when the foundation is rigid: $\tilde{T}_f$

$$\tilde{\varepsilon}_1 = \frac{1}{{R_f}^3}\varepsilon_1 + \varepsilon_f \quad \textbf{(4)}$$

Where

$\tilde{\varepsilon}_1$: The effective damping factor

ε_1= 5% for OBE, 7% for MCE (5% was used in this study)

ε_f: added damping ratio due to dam-foundation rock interaction

$R_f = \frac{\tilde{T}_f}{T_1}$

After calculating the effective damping factor for each model, its corresponding Rayleigh damping coefficients (α and β) were chosen such that the damping ratio was equal to the effective damping factor at the first three natural vibration frequencies of the system.

Frequency domain solution for the transient motion problem was conducted using the software EAGD for the 2D setting.

3.5. 2D SSI MODEL

In order to obtain theoretically robust solutions for 2D SSI models, the software EAGD was used with the user interface developed by Yücel [34]. This software includes the rigorous modeling of the soil-structure interaction effects by including the frequency dependent impedance matrices in the calculation procedure. The transient analysis of the concrete gravity dam was conducted in the software. A user defined input motion was applied as the base excitation. The software assumes the foundation beneath the dam body to be a half-space and solves the system in the frequency domain. In this study this software was used to obtain the robust solution of the 2D dam system to the pulse input in order to obtain its transfer function with the procedure described above.

The following input parameters are required by the software to conduct the analysis:

-Material Properties of the Dam Body:

Elastic Modulus
Mass density
Poisson's ratio
Hysteretic damping coefficient
Tensile strength

-Material Properties of the Foundation

Elastic Modulus
Mass density
Damping coefficient
Friction coefficient between dam and rock
Cohesion stress

-Geometric Properties of the Dam

Height below crest region (H1)

Height of crest region (H2)

Depth of reservoir (H_W)

Length of crest (Lc)

Upstream slope (m1)

Downstream slope (m2)

Crest downstream slope (m3)

-Dynamic Response Parameters

Input motion

Ground motion direction

Exponent of FFT algorithm

Time step (dt)

Wave reflection coefficient (α)

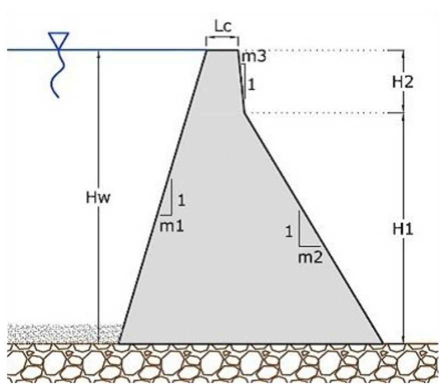

Figure 3.7 - Dam Geometry, EAGD Model

3.6. TIME HISTORIES USED IN RESPONSE ANALYSIS

Transient analyses were conducted in the fashion described above in order to obtain a quantitative comparison between the 2D SSI and 3D massless models. A total of 70 ground motions (35 ground motion pairs) were used for this purpose. [35] A ground motion suite was used in this study. This ground motion suite was used in many other studies [37,38] for the evaluation of ground motion selection and scaling techniques. The suite was prepared by O'Donnell and coworkers [39] who distinguished the earthquake records by means of their characteristic properties related to source, directivity, site and basin effects. The suite includes cyclic versus impulsive records, records with high, mid, or low frequency content, short or long duration records. Frequency domain analyses were utilized to investigate basin, duration, and pulse attributes of the records by the authors. Near fault motions (having a maximum fault distance of 20km.) were preferred for compiling the suite. The ground motions records were taken from PEER Ground Motion Database.

The properties and acceleration time histories of these records are presented in Table 3.1 and Figure 3.8, respectively. The ground motions were used in pairs when required in directions perpendicular and parallel to the dam axis.

Table 3.1 – Properties of Selected Motions

ID	Event	Date	PGA (g)	PGV (cm/sec)	Magnitude	Rjb (km)	Rrup (km)	V_{s30} (m/s)	Station	File ID
1	Loma Prieta	1989	0,526	41,92	6,93	3,9	10,7	376,1	BRAN	BRN090
2	Loma Prieta	1989	0,529	35,014	6,93	8,7	15,2	288,6	Capitola	CAP000
3	Loma Prieta	1989	0,644	55,148	6,93	0,1	3,9	462,2	Corralitos	CLS000
4	Loma Prieta	1989	0,106	8,767	6,93	39,3	39,5	367,6	Fremont - Mission San Jose	SJTE225
5	Loma Prieta	1989	0,357	28,616	6,93	9,2	10	729,6	Gilroy - Gavilan Coll.	GIL067
6	Loma Prieta	1989	0,284	41,964	6,93	10,3	11	338,5	Gilroy - Historic Bldg.	GOF160
7	Loma Prieta	1989	0,367	32,907	6,93	10,4	11,1	270,8	Gilroy Array #2	G02000
8	Loma Prieta	1989	0,555	35,684	6,93	12,2	12,8	349,9	Gilroy Array #3	G03000
9	Loma Prieta	1989	0,417	38,755	6,93	13,8	14,3	221,8	Gilroy Array #4	G04000
10	Loma Prieta	1989	0,17	14,175	6,93	17,9	18,3	663,3	Gilroy Array #6	G06090
11	Loma Prieta	1989	0,587	47,042	6,93	0	3,9	477,7	LGPC	LGP090
12	Loma Prieta	1989	0,512	41,151	6,93	7,6	8,5	370,8	Saratoga - Aloha Ave	STG000
13	Loma Prieta	1989	0,332	61,54	6,93	8,5	9,3	370,8	Saratoga - W Valley Coll.	WVC270
14	Loma Prieta	1989	0,386	15,396	6,93	12,2	18,5	714	UCSC	UC2090
15	Loma Prieta	1989	0,45	18,669	6,93	12	18,4	714	UCSC Lick Observatory	LOB000
16	Loma Prieta	1989	0,672	34,98	6,93	11	17,5	376,1	WAHO	WAH090
17	Cape Mendocino	1992	1,497	125,133	7,01	0	7	513,7	Cape Mendocino	CPM000
18	Cape Mendocino	1992	0,116	29,934	7,01	16	19,9	457,1	Fortuna - Fortuna Blvd	FOR000
19	Cape Mendocino	1992	0,662	89,684	7,01	0	8,2	712,8	Petrolia	PET090
20	Cape Mendocino	1992	0,549	41,875	7,01	7,9	14,3	311,8	Rio Dell Overpass - FF	RIO360
21	Kobe- Japan	1995	0,042	5,306	6,9	158,1	158,6	256	FUK	FKS090
22	Kobe- Japan	1995	0,821	81,302	6,9	0,9	1	312	KJMA	KJM000
23	Kobe- Japan	1995	0,503	36,623	6,9	7,1	7,1	609	Nishi-Akashi	NIS090
24	Kobe- Japan	1995	0,243	37,795	6,9	19,1	19,1	256	Shin-Osaka	SHI000
25	Kobe- Japan	1995	0,694	85,298	6,9	0	0,3	312	Takarazuka	TAZ090
26	Kobe- Japan	1995	0,616	120,73	6,9	1,5	1,5	256	Takatori	TAK090
27	Duzce- Turkey	1999	0,822	62,101	7,14	12	12	326	Bolu	BOL090
28	Duzce- Turkey	1999	0,535	83,506	7,14	0	6,6	276	Duzce	DZC270
29	Duzce- Turkey	1999	0,111	14,204	7,14	0,2	0,2	424,8	Lamont 1058	1058-E
30	Duzce- Turkey	1999	0,147	11,978	7,14	4,2	4,2	424,8	Lamont 1059	1059-N
31	Duzce- Turkey	1999	0,134	13,685	7,14	11,5	11,5	481	Lamont 1061	1061-E
32	Duzce- Turkey	1999	0,257	16,313	7,14	9,2	9,2	338	Lamont 1062	1062-E
33	Duzce- Turkey	1999	0,97	36,501	7,14	3,9	3,9	424,8	Lamont 375	375-N
34	Duzce- Turkey	1999	0,159	12,953	7,14	8	8	659,6	Lamont 531	531-N
35	Hector Mine	1999	0,337	41,743	7,13	10,3	11,7	684,9	Hector	HEC090

Figure 3.8 – Acceleration Times Histories of Selected Motions

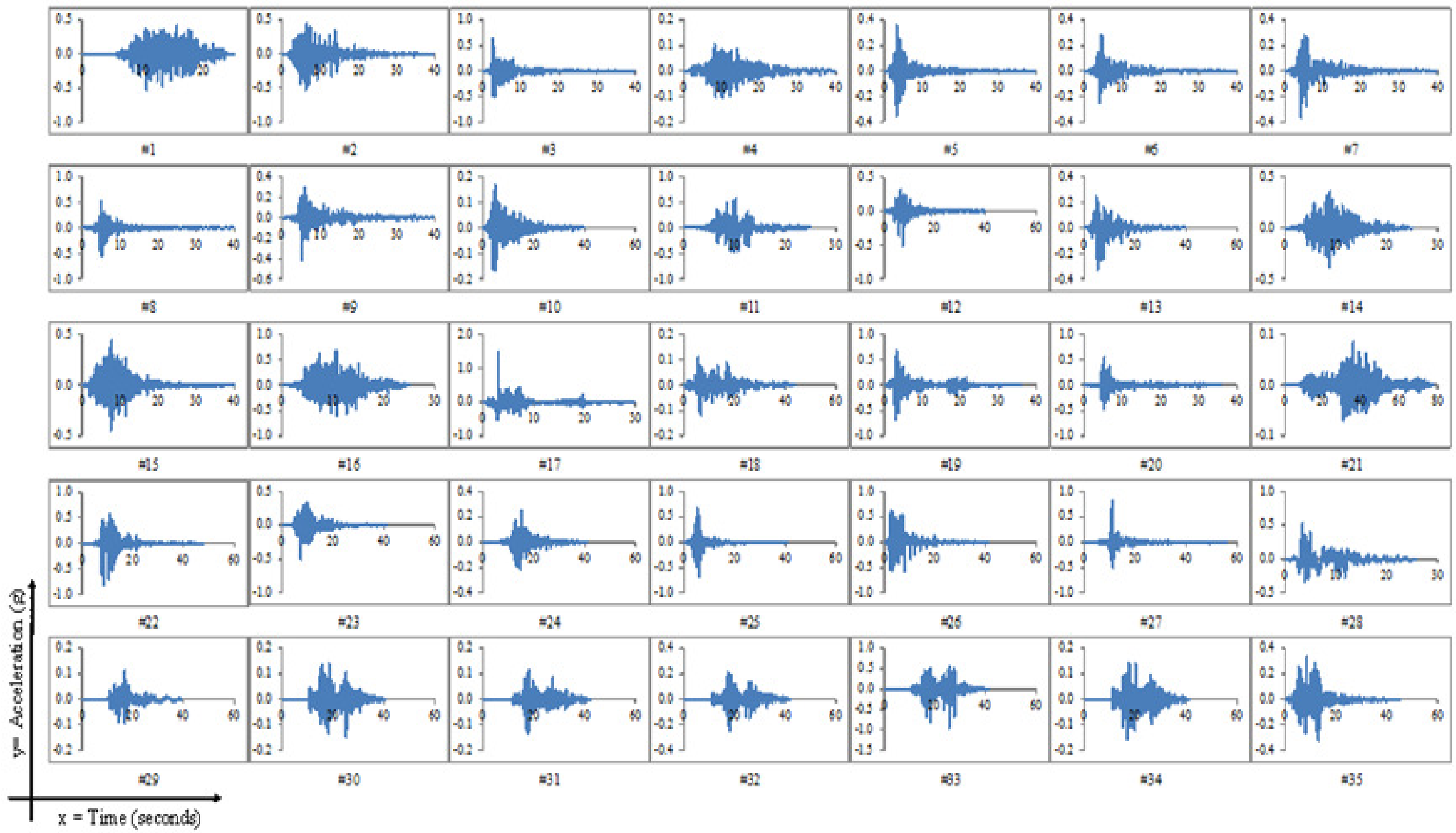

CHAPTER 4

2D/3D RESPONSE OF GRAVITY DAMS

4.1. FREQUENCY RESPONSE FUNCTIONS

The comparison of the 2D and 3D response of gravity dams were conducted in this section using the frequency response functions for the crest acceleration at the middle of the dam. In order to investigate the effect of valley width on the 3D response of a given system, an identically shaped gravity dam section was assumed to be built in five different valley settings denoted as 0x, 1x, 2x, 4x, and 10x as described above. For the purpose of investigating the effect of the construction joints on the behavior, two different models were used. The first one represented a monolithic construction (monolithic), in which the construction joints were not modeled (i.e. representing either zip-like joints, partially cut sections or calcified, filled in joints for older systems). The second model incorporates an ideal monolith behavior in accordance with the 2D modeling assumptions of gravity dams: the monoliths were modelled completely independent of each other and are connected solely at the foundation. The model is an idealization assuming no contact forces are transferred between the monoliths and the pounding between adjacent monoliths was also not considered (which is investigated later in the study). Response of the dam was considered only in the transverse direction (perpendicular to the axis of the dam) in these analyses.

The 2D SSI model was constructed using the software EAGD as described before. Identical material properties were used in the 2D and 3D models except for the specialization of damping. Rayleigh damping was used in the 3D model along with the massless foundation assumption in order to reflect the damping provided by the soil-structure interaction on the system. This effect is intrinsically included in the EAGD solution due to the robust, frequency domain solution of the SSI problem.

The ratio of the foundation stiffness to the concrete stiffness was varied for each model, ranging from 0.5 to 4.0. The hysteretic damping coefficient for the foundation was assumed as 0.1 while the damping ratio for the dam body was assumed as 5% for the EAGD models. The geometry of the 2D model was defined such that it matched the dam cross section of a full size monolith of the 3D models.

The following material properties were used for the models.

Table 4.1 – Material Properties

Property	**2D SSI**	**2D MF**	**3D MF**
Elastic Modulus of Concrete (MPa)	20,000	20,000	20,000
Mass Density of Concrete (kg/m^3)	2,400	2,400	2,400
Damping Ratio of Concrete	0.05	Varies	Varies
Mass Density of Foundation (kg/m^3)	2,500	0	0

The frequency response functions for the monolithic idealization of the system is compared in Figure 4.1 for the MF models for varying foundation/dam stiffness ratio (E_f/E_c). The response from typical 2D design models, i.e. a 2D massless foundation model with equivalent damping as well as the 2D rigorous SSI solution obtained using EAGD is also provided on the same plot. A similar figure for the independent idealization of the monoliths is presented in Figure 4.2. The response from 3D models are compared to the aforementioned 2D models in this plot as well.

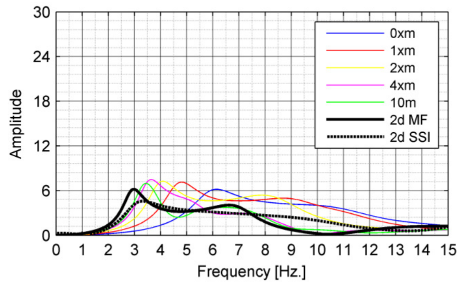

(a) E_f/E_c=0.5

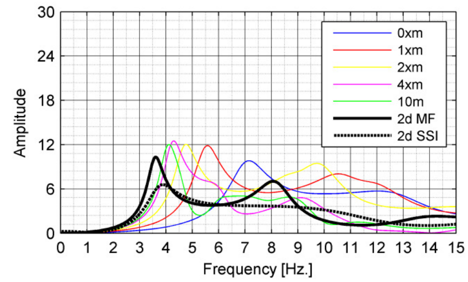

(b) E_f/E_c=1.0

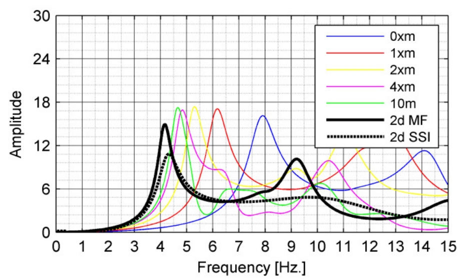

(c) E_f/E_c=2.0

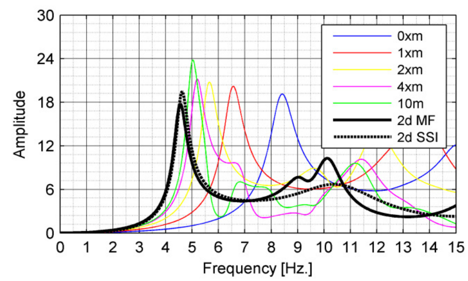

(d) E_f/E_c=4.0

Figure 4.1 – Frequency Response Functions for Monolithic 3D and 2D Models

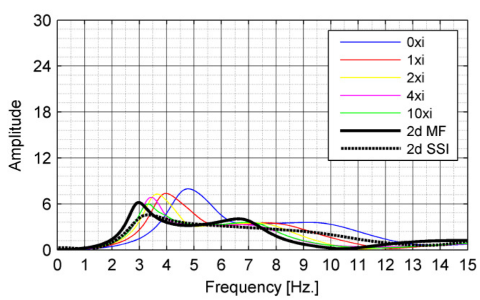

(a) E_f/E_c=0.5

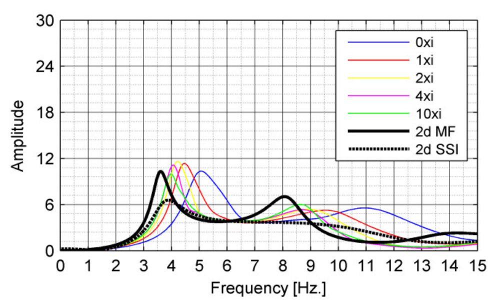

(b) E_f/E_c=1.0

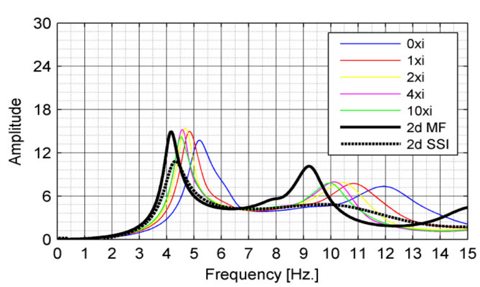

(c) E_f/E_c=2.0

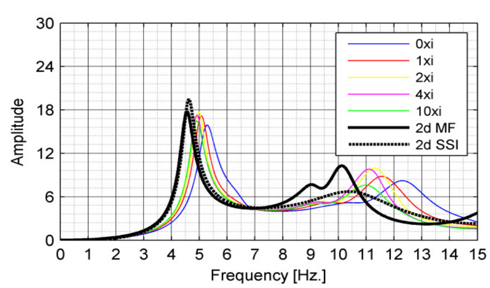

(d) E_f/E_c=4.0

Figure 4.2 - Frequency Response Functions for Independent 3D and 2D Models

Investigation of the frequency response functions given in these figures show:

1) There was a significant difference in the natural frequency between the 2D models and the 3D models, even for a valley width of ten times the dam height for a monolithic gravity dam system. The difference in the fundamental frequency was valid for all ranges of the foundation to dam stiffness.
2) There was a surprising difference in the natural frequency estimate between the 2D models and the 3D models even for the independent monolith idealization. However, as expected, this disparity reduced for increasing foundation stiffness and valley widths.

The reduction in the peak of the frequency response, as commonly expressed by the equivalent damping ratio at the fundamental frequency, was predicted on the conservative side using 2D massless models. For some 3D massless models, this trend appeared to be valid, while for others it was not.

The figures shown above allow for a qualitative basis for the comparison of the frequency response function of the 2D and 3D solutions. Quantitative comparison is sought in the next section.

4.2. 2D/3D BEHAVIOR

For the quantitative comparison of the response functions given in the previous figures, first, the differences in the fundamental frequency were computed. As given above, the frequency response functions for the monolithic idealization of the dam system implied a significant difference in the fundamental frequency compared to 2D models with decreasing valley width. For the massless models, at a valley width of 10x the height of the dam, the fundamental frequency of the 3D system was still 10% higher than the 2D rigorous model. The difference in the fundamental frequency between the 2D and 3D models was amplified by 10% by the decrease in the ratio of the foundation/structure modulus ratio: i.e. softer foundation media corresponded to

3D models yielding much higher fundamental frequency values compared to 2D models.

In terms of the fundamental frequency, the difference between the 2D and 3D modeling appears to be significant for the monolithic dam model. For instance, for a relatively wide valley width at four times the dam height (4xm), the fundamental frequency of the 3D model was still 40% more than its counterpart obtained from the 2D idealized solution at the same foundation/dam stiffness ratio. A 2D analysis could hardly be justified to predict the performance of such a system given the large difference in the fundamental frequencies of these systems.

Table 4.2 - Percent Difference in Fundamental Frequency, 3D vs 2D Models (Positive Values Imply that the 3D Model Has a Higher Frequency)

		3D MF vs 2D SSI							
		Independent				**Monolithic**			
		E_f/E_c							
		0.5	**1.0**	**2.0**	**4.0**	**0.5**	**1.0**	**2.0**	**4.0**
MODEL	**0x**	45.25	30.7	20.45	14.15	86.78	84.81	83.66	82.14
	1x	20.3	15.19	12.22	9.79	45.81	43.99	43.32	41.93
	2x	10.43	8.7	8.52	7.8	23.84	22.94	23.01	22.35
	4x	4.28	5.06	6.25	6.35	10.24	10.6	12.07	12.3
	10x	0.74	2.85	5.11	5.95	4.47	6.17	8.1	8.73

For the idealization with independent monoliths, the difference between the fundamental frequency of the 2D and the 3D models decreased to some extent. For V/H ratio at 10, the fundamental frequency obtained from 3D models were similar to their 2D counterparts, with the disparity only visible at the high end of E_f/E_c ratios. For systems in narrow valleys, the difference in the fundamental frequencies was still significant. At the E_f/E_c ratio of 0.5, the natural frequency of a 3D model with independent monoliths was 30% higher than a 2D counterpart, showing significant coupling occurring between the monoliths due to kinematic soil-structure interaction. Monoliths could not move indepedently from each other, even seperated at the joints, as their motion was constrained at the base by the common boundary. The coupling at the base, hence the difference in the fundamental frequency between the 2D and 3D models, was significantly reduced by an increase in the foundation modulus rendering each monolith independent of each other.

In conclusion, even with the assumption of perfectly severed joints, coupling between monoliths due to common foundation boundary condition appears to be possible. The difference in the fundamental frequency between 2D and 3D modeling approaches could still be significant provided that the dam is built on a flexible foundation.

4.3. EFFECT OF SOIL STRUCTURE INTERACTION ON THE FREQUENCY RESPOSE

Increased damping in the overall response is perhaps the most recognized effect of the soil-structure interaction phenomenon for gravity dams. Hence the peak of the response quantity can be interpreted as a comparison index for the effective damping in the response at the natural frequency of the system. The increase in damping is reflected by the lowering of the overall response quantities in the frequency domain.. With the decrease in the V/H ratios (valley width decreasing), the discrepancy in the peak of the response for the 2D and 3D models at the fundamental mode becomes more apparent (as well as the change in the modal frequency). For example, for a V/H ratio of 1 and E_f/E_c=0.5, the peak of the response obtained from a 3D solution was 50% higher than the rigorous 2D solution. On the other hand, the peaks obtained from the 2D and the 3D massless foundation solutions were similar as expected due to the equivalent damping ratio assumption. Absent a rigorous 3D SSI model, the comparison of the massless models and the SSI models can be conducted at a V/H ratio of 10, yielding the conclusion that for softer foundations, the equivalent damping ratio suggestion based on SDOF solution [9] leads to conservative damping ratios. Considering SSI rigorously, the response is substantially lower. The effect was naturally reduced for stiffer foundations.

The difference between the equivalent damping ratios of the 3D MF and 2D SSI models are presented in Table 4.3. The damping ratios for the massless models were obtained as given in section 3.3 (Appendix A) while their 2D SSI counterparts were calculated using half-power bandwidth method (5) from Figure 4.1 and Figure 4.2.

$$\xi = \frac{f_b - f_a}{2f_n} \tag{5}$$

Where ξ is the damping ratio, f_a and f_b are the frequencies corresponding to an amplitude of $1/\sqrt{2}$ times the amplitude at the peak, and f_n is the first natural vibration frequency of the model which corresponds to the peak amplitude.

Table 4.3 - Percent Difference in the Damping Ratio in First Mode, 3D vs 2D Models (Negative Values Imply That Damping for 2D SSI Model Is Larger)

		3D MF vs 2D SSI							
		Independent				**Monolithic**			
		E_f/E_c							
		0.5	**1.0**	**2.0**	**4.0**	**0.5**	**1.0**	**2.0**	**4.0**
MODEL	**0x**	-61.33	-43.87	-19.64	25.83	-65.41	-52.11	-30.83	14.04
	1x	-64.45	-50.56	-27.77	16.00	-65.41	-51.59	-30.83	14.04
	2x	-65.41	-52.11	-31.84	12.07	-65.41	-52.11	-31.84	12.07
	4x	-65.90	-53.14	-32.86	10.10	-65.90	-53.14	-32.86	10.10
	10x	-62.05	-44.90	-20.65	25.83	-66.38	-53.65	-33.88	8.14

The comparison of the damping ratio values as given above showed that the proposed damping suggested in [7] is mostly on the conservative side.

4.4. TIME DOMAIN EFFECTS

The comparison of the frequency response parameters is effective only to an extent in identifying the different behavior of the chosen models. While comparing the peak response values (or equivalent damping), the location of the frequency is inadvertently ignored. The effects of the discrepancy in both the frequency and damping can only be simplified to a single comparative index in the time domain analysis. The consideration of the response in the time domain is also essential as almost of all our engineering decision parameters (except perhaps the fundamental frequency) are based on the time domain parameters. Naturally, the uncertainty due to variation in the ground motions has to be reflected in these analyses quantifying the effect of the different frequency responses on time domain parameters.

In order to predict the difference in the time domain response parameters for different model idealizations, the frequency response functions were used in accordance with the procedure given in Section 3.4. along with 35 different pairs of ground motions as the input time histories. The response quantity chosen was the top displacement of the dam, as this quantity was expected to be highly correlated with the common response parameters of interest such as the base shear, maximum stress, etc. In this fashion, the quantitative difference statistics between the modeling approaches were obtained for a range of ground motions which can help the designers predict an expected difference of their own predictions.

Engineers usually utilize 2D tools for relatively simpler but quicker analyses of dams. The disparity in the prediction of these simpler analysis with regard to the 3D analysis results was using (6). In order to compare corresponding quantities, the comparison was made between the massless models, so that only the effect of the 2D vs 3D modeling was reflected on the quantity.

$$\varepsilon(\%) = \frac{\max|2D_{MF}| - max|3D_{MF}|}{\max|3D_{MF}|} x100 \qquad \textbf{(6)}$$

The mean value as well as ± standard deviation of the differences between the 2D and 3D results are presented in Figure 4.3 and Figure 4.4. For example, as given in Figure 4.3, a 2D model can predict the top displacement by as much as 90% over and 50% under for a E_f/E_c ratio of 0.5 and the V/H ratio of 1.0. The difference in the analyses results reduces significantly for $E_f/E_c=4.0$, i.e. fixed dam condition, as given in Figure 4.3 and Figure 4.4. It was interesting to observe that the difference in the fundamental frequency between the idealizations can significantly affect the results as such. The frequency content of the motions', coupled with the system's dynamic properties, favored the 2D models more. The results of the 2D analyses were clearly higher than the 3D analyses for a large number of cases although the damping ratio of the 2D models (i.e. such as the response peaks from Figure 4.1a-c) were somewhat larger.

It can also be seen that the time domain solutions from 2D models with varying ground motions yielded widely varying results which ranged from 0% to up to 100% disparity with respect to the 3D solution. The standard deviation of the results decreased as the valley width increased. The results depend heavily on the frequency content and the amplitude of the ground motion as well.

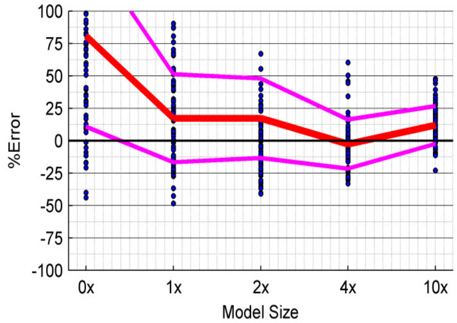

(a) E_f/E_c=0.5

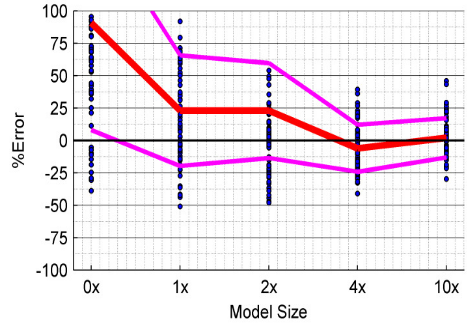

(b) E_f/E_c=1.0

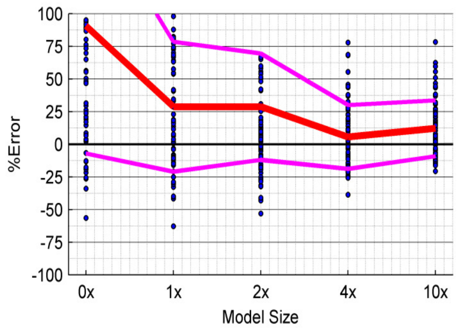

(c) E_f/E_c=2.0

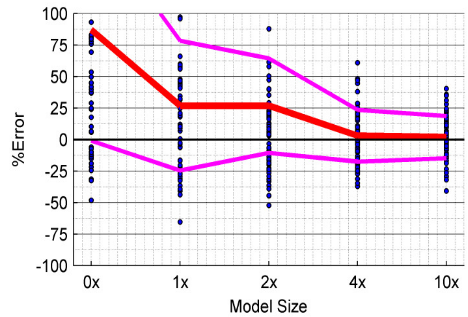

(d) E_f/E_c=4.0

Figure 4.3 - Difference in Time History Results, Monolithic Systems (Blue: Individual Motions, Red: Mean, Magenta: Mean $\pm\sigma$)

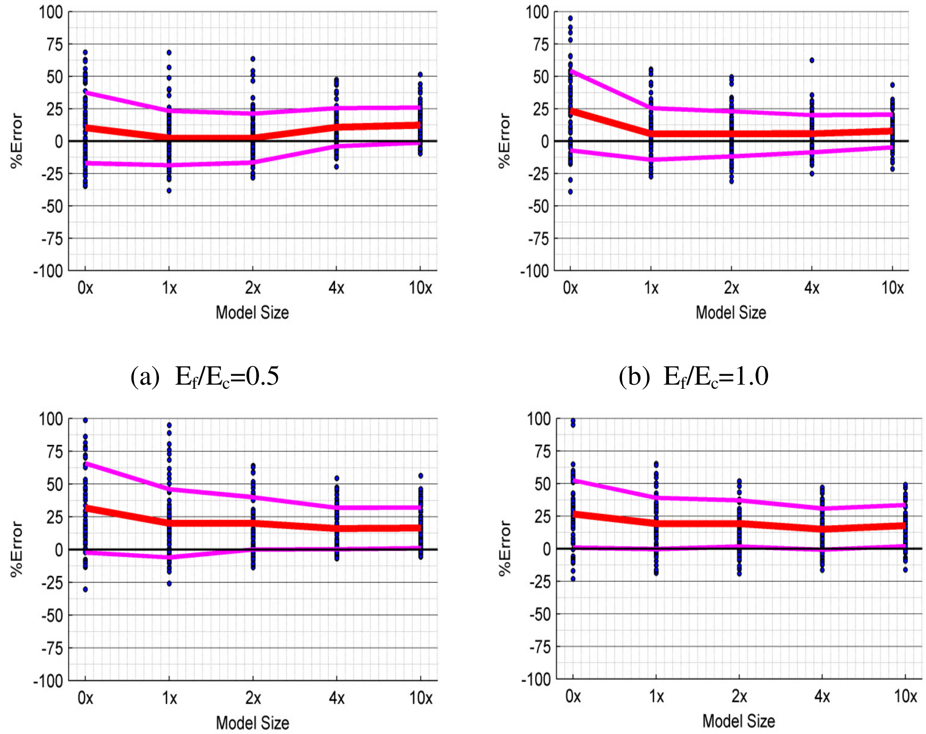

(a) E_f/E_c=0.5 (b) E_f/E_c=1.0

(c) E_f/E_c=2.0 (d) E_f/E_c=4.0

Figure 4.4 - Difference in Time History Results, Independent Monolith Systems (Blue: Individual Motions, Red: Mean, Magenta: Mean ±σ)

As given above, given a time history, the results of a 2D prediction could be significantly different than the 3D counterparts. Most of the time this was remediated in the mean quantity: for example, for an independent system with V/H ratio of 4 and E_f/E_c=1, as much as 60% difference in prediction was possible, although the mean difference for 70 different ground motions was lower than 10%. 2D analyses can be conducted much faster than 3D analysis, therefore, the discrepancy in the individual analysis results could be amended for the final choice using a set of ground motions and multiple analyses. However, the user would need the number of motions required to get an appropriate correspondence with the 3D analysis, the condition being that the mean from the 2D analyses predicts the 3D analysis exactly or more conservatively. For the models with different valley widths, and the monolithic and independent dam conditions, the number of motions required for a 2D analysis was sought by obtaining the distribution of the mean of the results of a number of (n) chosen motions from the set of 35 motions. (Only the first motion of each pair was used due to computational limitations.) The well-known clause in ASCE 7-10 document indicates that the mean of the analyses for 7 different ground motions is adequate to establish a design quantity from time history results. The distribution of the results of ground motions with 3 to 7 time histories selected from the 35 motions provided in Table 3.1 can be found in Figure 4.5.

Table 4.4 – Number of Combinations

Number of Motions Chosen	# of Combinations
3/35	6,545
4/35	52,360
5/35	324,632
6/35	1,323,160
7/35	6,724,520

A combination was considered a poor estimate if the mean of the % differences between the 2D and 3D solutions fall below -5%. The x-axes in Figure 4.5 indicate the number of motions in each combination and the y-axes indicate the percent of combinations which are poor estimates. Therefore lower numbers in the y-axes of these plots indicate a better estimation to the 3D model. For example for the model 4xi and E_f/E_c= 1.0; the mean difference of around 30% percent of the 1-motion combinations fell below -5%, around 18% of the 2-motion combinations fell below -5% and around 10% of the 3-motion combinations fell below -5% etc.

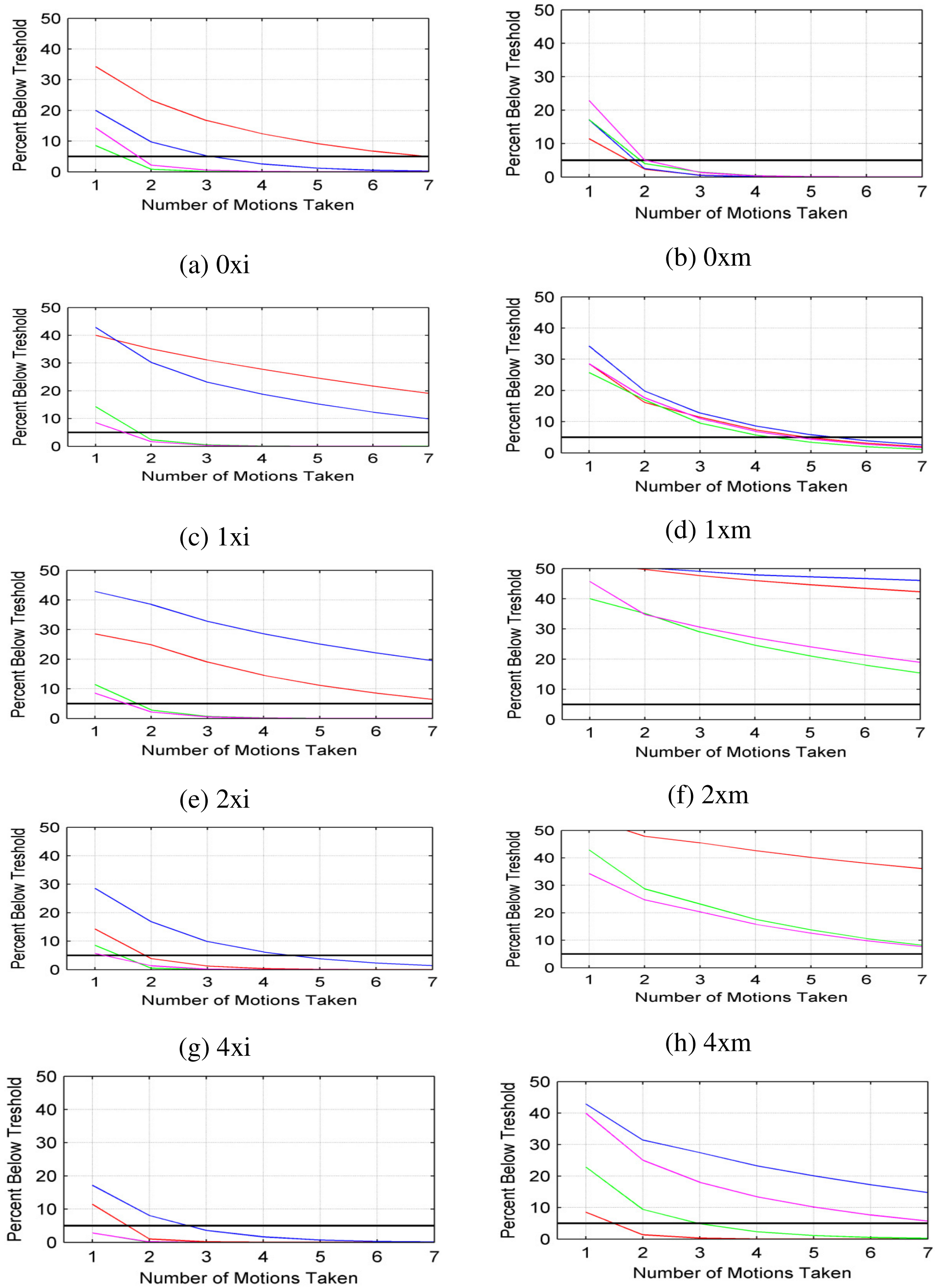

(a) 0xi (b) 0xm

(c) 1xi (d) 1xm

(e) 2xi (f) 2xm

(g) 4xi (h) 4xm

(i) 10xi (j) 10xm

Figure 4.5 - Distribution of 2D/3D Disparity with Given Combinations (Different colors represent E_f/E_c values where: Red= 0.5, Blues=1.0, Green=2.0, Magenta=4.0, The Black Line represents 5% Mark)

5% was taken as an acceptable limit for the percent of combinations which yielded poor estimates. This limit is represented by a horizontal line in the figure. The results showed that in general independent monolith results tended to yield very low mean differences when higher number of motion combinations were chosen. The monolithic models however, yielded large differences even when combinations of 7 motions were selected. This was expected since the standard deviations in the % difference for independent monolith systems were smaller than those of monolithic models. The combinations produced better results in narrow valleys for monolithic models. This however is not an indication of the 2D assumption better estimating 3D conditions in narrow valleys and was due to the 2D solution greatly overestimating its 3D counterpart in most of the cases as seen in Figure 4.3. The 2D solution, was significantly conservative and did not seem to yield a good estimation for the 3D case. Fully monolithic dam bodies were not suitable for the plane-stress or plain-strain assumptions of the 2D modeling.

CHAPTER 5

EFFECT OF JOINT PROPERTIES ON SYSTEM PERFORMANCE

Instead of the fully free or fixed idealization of the joints between monoliths utilized in the previous sections, a more realistic point of view was taken in this section in order to investigate the effect of possible joint behavior on the system. The main purpose was to evaluate the function of sliding and friction on the performance of a given dam system which is separated to form distinct monoliths. This type of modeling represents poorly cut construction joints or grouted or calcified joints which prevents each monolith from acting independently.

5.1. RESERVOIR EFFECT

A dam with full reservoir was considered in this part of the study where the effects of joint properties were investigated. In order to account for the contribution of a reservoir to the dynamic response of the system, Westergaard added mass method [1] was used in addition to the hydrostatic load on the upstream face. This method provides a mass distribution along the upstream face provided by the following equation.

$$\mu = \frac{7}{8}\rho_f\sqrt{(H(H-X))} \tag{7}$$

Where ρ_f is the fluid density, H is the distance in the gravity direction between the bottom of the reservoir and the fluid surface, and X is the distance in the gravity direction between any chosen point below the fluid surface and the bottom of the reservoir.

The added masses were applied to the model using one-node mass elements (denoted as PT3T in the Diana software) that act as concentrated masses on the upstream face, with the magnitude of this mass calculated using (7) for each node at the front surface.

5.2. THE EFFECT OF INTERFACE PROPERTIES ON MONOLITH BEHAVIOR

In order to determine the limits of sliding on the interfaces for a dam monolith, incremental dynamic analysis was chosen as the tool to determine how the properties of the motion should affect the interface behavior. For a selected motion, incremental dynamic analysis was conducted for the 240m wide model for assessing the effect of possible variations in the interface properties on the system response. The variations in the properties of the monolith to monolith interface can be significantly different based on the interface details, grouting material used, wear and tear in the expansion joints, as well as the development of calcification. The variation in the joint properties were expressed as changes to the cohesion and friction angle properties of the joint. Five different models were used to categorize these variations: 1) high cohesion, high friction model (grouted joint) 2) low cohesion, high friction model (non-grouted joint) 3) low cohesion-low friction model (non-grouted joint, poor connection) 4) low cohesion, medium friction model (non-grouted joint) and 5) The case where the interface has very low transverse stiffness (Independent Monoliths) The material properties used are presented in Table 5.1.

Table 5.1 – Joint Properties

Model	Transverse Stiffness (MPa)	Cohesion Coefficient (MPa)	Tangent of Friction Angle, tanφ
1	2.0e6	1.812	0.80
2	2.0e6	0.005	0.80
3	2.0e6	0.005	0.35
4	2.0e6	0.005	0.50
5	2.0e-3	-	-

The ground motion chosen was scaled to different levels for the incremental dynamic analysis (IDA). The original motion was selected such that the spectral acceleration corresponding to the first vibration frequency of the structure was close to 0.5g for 5% damping. This record was then scaled in order to obtain spectral acceleration values ranging from 0.2g to 1.0g. For example a scale of 0.375 (0.2/0.533) was applied to the record in order to obtain the record denoted as "0.2g", which yielded 0.20g spectral acceleration for the first vibration period of the model. The details, acceleration time history, and the acceleration spectrum (for 5% damping) of the selected motion is presented in Table 5.2 and Figure 5.1.

Table 5.2 - Selected Ground Motion for IDA

Event	Year	Station	Magnitude (M_w)	Fault Type	R_{jb}(km)	R_{rup}(km)	V_{s30} (m/s)
Victoria, Mexico	1980	Cerro Prieto	6.33	Strike-Slip	13.80	14.40	659.6

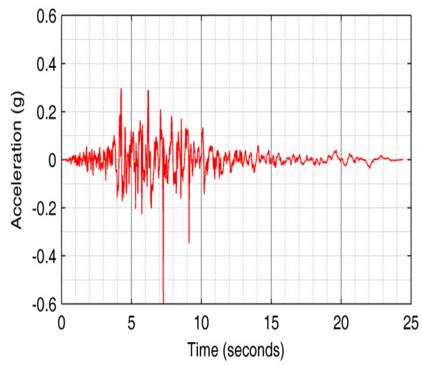

(a) Acceleration Time History

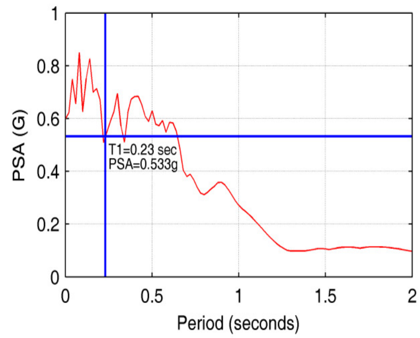

(b) Pseudo-Spectral Acceleration Spectrum

Figure 5.1 - Acceleration Time History and Response Spectrum of the Chosen Motion

The results of the incremental dynamic analyses have been compiled in terms of the maximum values of the selected demand quantities: the stresses at the heel, toe, and midzone of the dam, the base shear, and the crest acceleration of the monolith. The maximum value of the demand quantities observed during the analyses are then plotted against the spectral acceleration of the motion on the first vibration period of the model.

The heel, toe and midzone elements are chosen such that:

> Heels: Elements whose centroid falls inside the 20m x 20m x 20m portion of the 20m wide monolith at the bottom part of the upstream face.
>
> Toes: Elements whose centroid falls inside the 20m wide triangular prism at the bottom of the downstream face.
>
> Midzone: Elements whose centroid falls inside the 20m x 20m x 20m portion of the monolith at mid height of the upstream face

A visual representation of the selected areas are shown Figure 5.2.

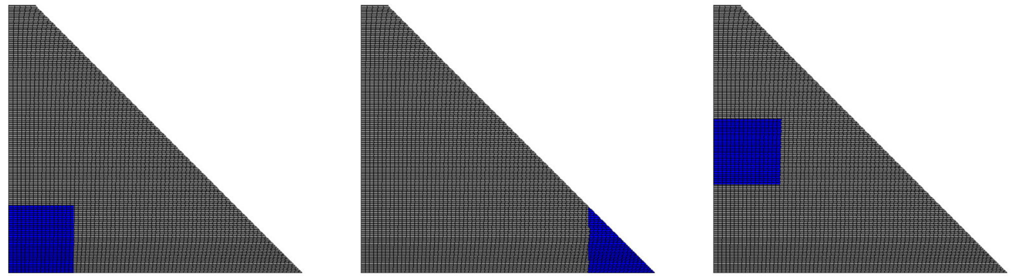

(a) Heel (b) Toe (c) Midzone

Figure 5.2 - Visual Representation of Heel, Toe, and Midzone Areas of a Monolith

For the heel and toe stresses, results obtained from the two different monolith types were considered for the 3D model, first monolith being on the slopes at the sides of the dam (denoted as “side”) and the other at the center of the dam. (Denoted “center”. For base shear and midzone stress, only the center monolith was considered. The crest acceleration was taken at the highest node of the center monolith at the downstream face. The base shear values were the maximum shear stress occurring in any part of the dam-foundation interface during the analysis. The results from the analyses were also compared with the 2D model for the comparison of the predictions from 2D and 3D approaches. The same motions (Scaled such that the motions yield the same PSA values for the 2D model) were applied to the 2D model and the same demand parameter values were obtained from these analyses. Sample time histories of different demand quantities for each type of model is presented in Figure 5.3, Figure 5.4, and Figure 5.5. Both the results from individual elements in the heel, toe, midzone and base areas and their mean values are presented in these figures.

0.2g **0.8g**

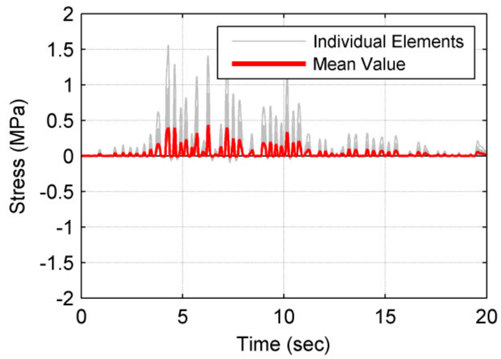

(a) 2D

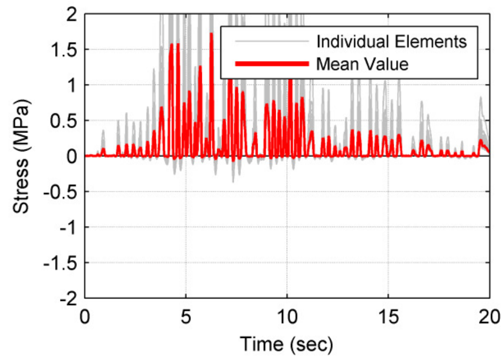

(b) 2D

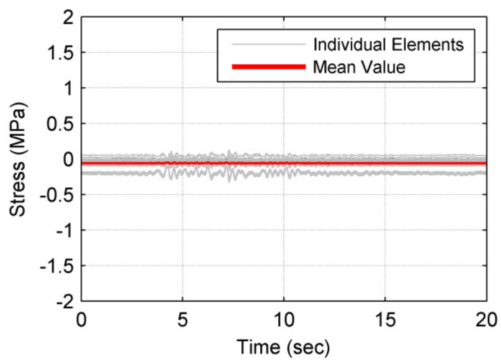

(c) 3D Independent

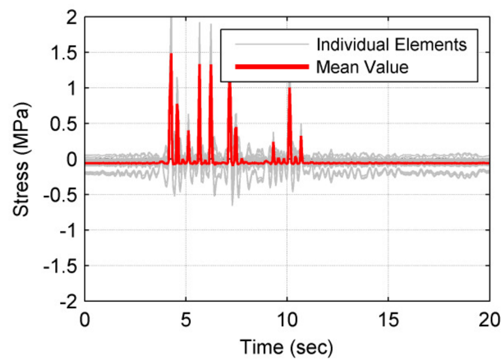

(d) 3D Independent

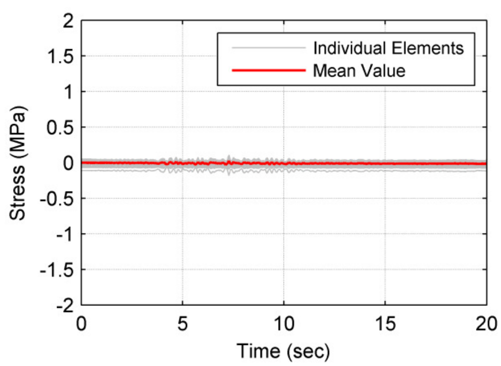

(e) 3D Friction

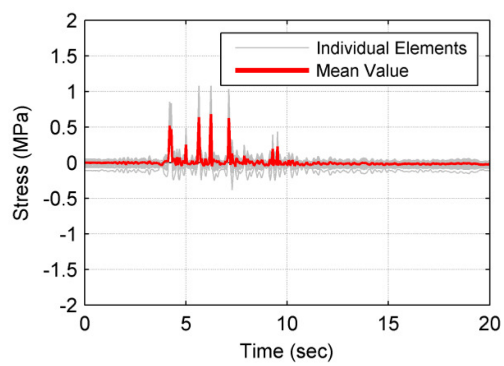

(f) 3D Friction

Figure 5.3 - Comparison of Toe Stress Time Histories (2D Model, 3D Independent, 3D Friction Model)

0.2g **0.8g**

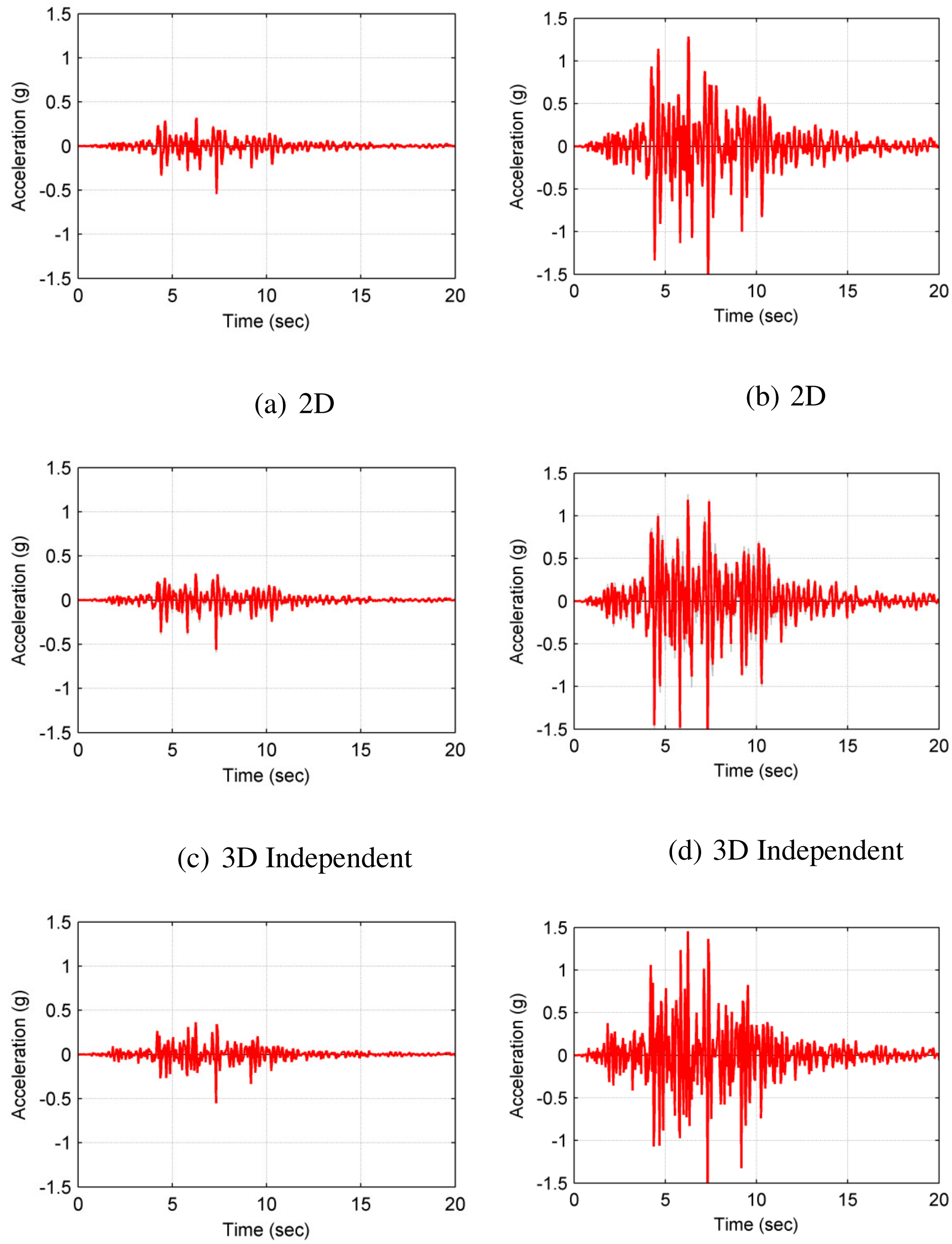

(a) 2D

(b) 2D

(c) 3D Independent

(d) 3D Independent

(e) 3D Friction

(f) 3D Friction

Figure 5.4 - Comparison of Crest Acceleration Time Histories (2D Model, 3D Independent, 3D Friction Model)

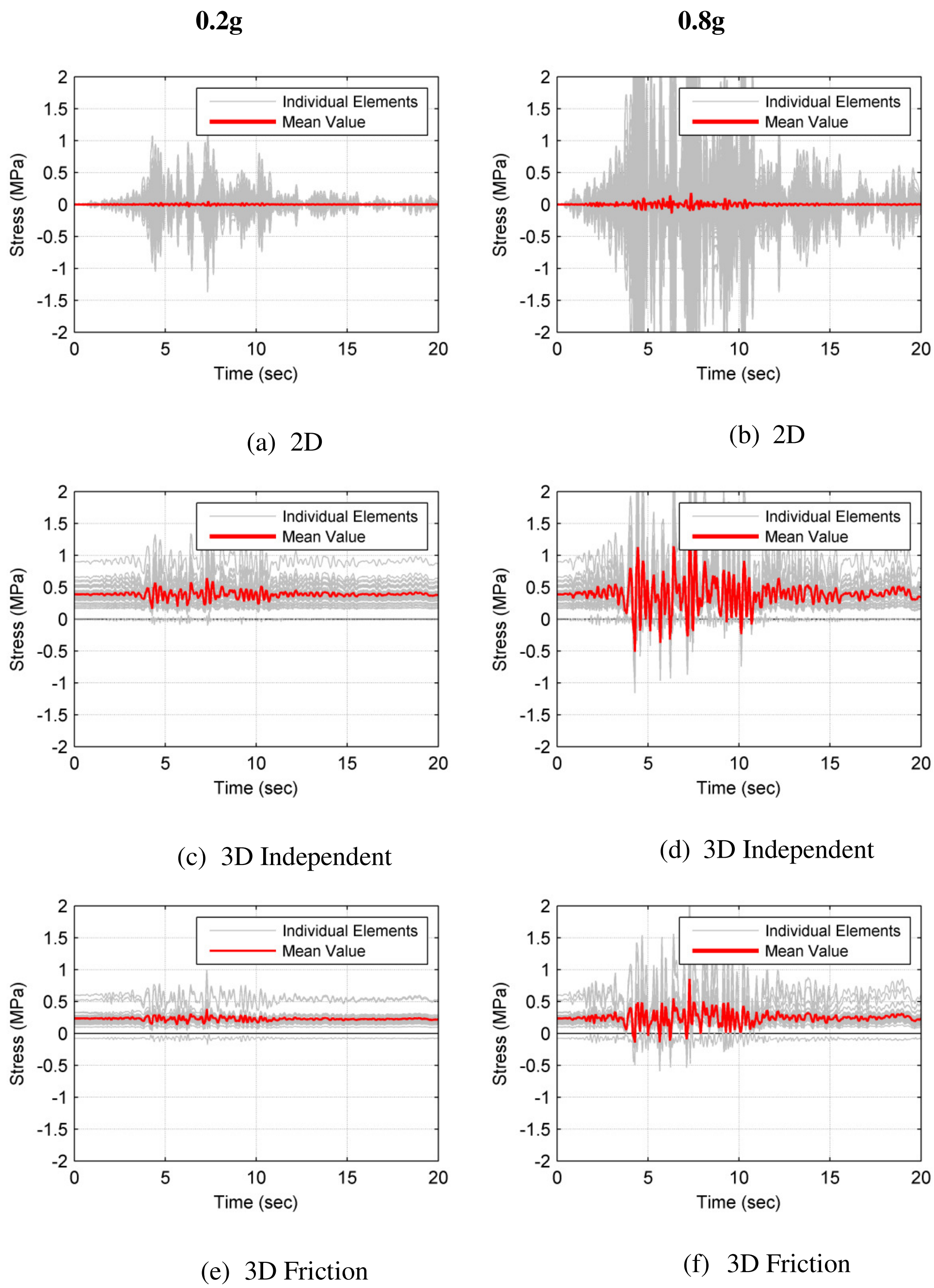

Figure 5.5 - Comparison of Base Shear Time Histories (2D Model, 3D Independent, 3D Friction Model)

The summary of the results compiled from the time history data for each response quantity are presented in

Figure 5.6. The results clearly indicate that even dramatic changes in the Coulomb friction parameters of the interface yielded close to no difference in the demand parameters. The increase in the ground motion intensity in most cases did not appear to create any non-linear slipping behavior in the interface elements. The transverse stiffness was the most effective parameter for the response of the system. However there is no singular pattern as to the conservativeness of the independent monolith solution when compared to the models with Coulomb Friction. While the independent monolith solution generally yielded greater values in the demand parameters this was not always the case, as in stresses found in heels of side monoliths. When 2D model was added to this comparison, it can be seen that the 2D model always overestimated the Coulomb Friction model save for the crest acceleration, in which all models yielded similar results. The independent monolith model produced similar results to the 2D solution as expected. As for the toe and heel stresses, the 2D solution yielded closer estimates to the 3D solutions in the center monoliths where the geometry of the cross section is constant throughout the length of the monolith, whereas it significantly overestimated the demand quantities on the side monoliths.

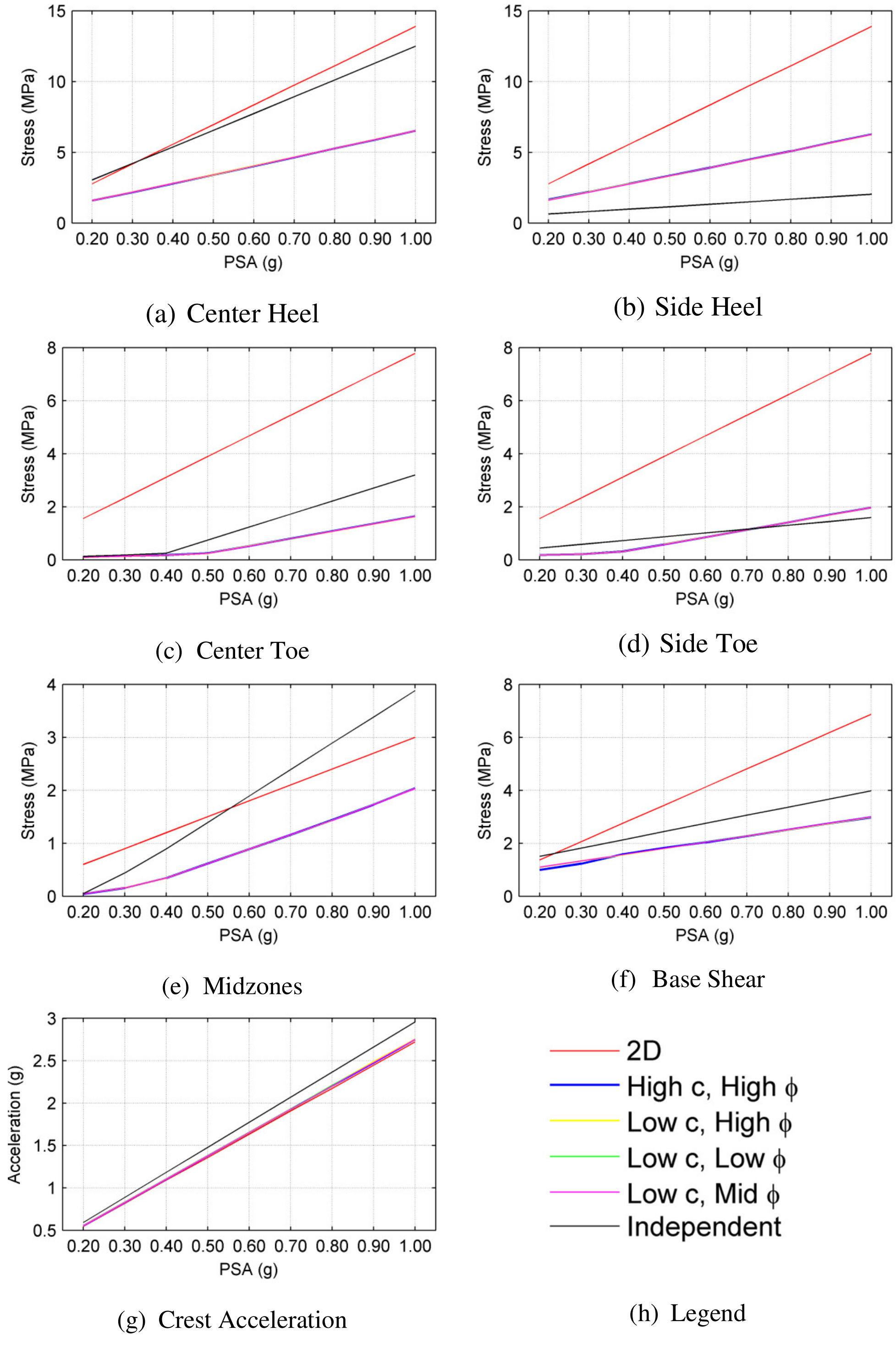

Figure 5.6 - The Effect of Interface Properties on Seismic Demand Parameters for the 240m Wide Model (2D, 1, 2, 3, 4, and 5)

5.3. JOINT OPENING/CLOSING BETWEEN MONOLITHS

The distance between the monoliths forming a dam system is one of the parameters that define the interface in such systems. Independent monoliths are usually built with a gap in between the monoliths, the flow between the monoliths obstructed by the help of water stoppers or grouting on the upstream side of the dam. While the formwork has been responsible for the formation of the monolith spacing in older systems, diamond saw cutting is the usually preferred choice in RCC for severing the dam body for expansion joints. However, the distance provided for this purpose is hardly analytically selected. In order to investigate the possible closing of joints with relation to this distance and the importance of this effect on the system behavior, a range of analyses were conducted to ascertain the effect of joint width necessary to avoid the closing and pounding of the interface.

Time history analyses were conducted on the model with 240m valley width by applying bi-directional earthquake acceleration to the system. The movement parallel to the axis of the dam would lead to the closing of this gap, which could also create coupling between the behaviors of independent monoliths. In order to investigate the possibility of such a behavior for different joint openings, 35 sets of two perpendicular components of the ground motion records were applied to the model and the displacements of the interface elements parallel to the dam axis were obtained. In order to ascertain the closing of the gap does not have an effect on the monolith behavior, two different ratios were defined. First, the ratio of the time the displacement at the interface exceeding the gap value was computed from each time history pertaining to the interface elements. In addition to this temporal quantity, a spatial quantity for gap closing was defined as the ratio of the elements between two monoliths in which the gap displacement was exceeded during the ground motion. The ratio of the time to the total duration of the ground motion that a given percentage of joint members were closed were calculated for assumed joint widths for each ground motion pair. Joint widths varying from 0 to 5 cm were evaluated for adequacy allowing a limited portion of the gap (spatially) to be closed at any time during the motion.

The resulting plots were obtained by applying the unscaled motions as well as by scaling the motions by a factor of 2 in order to include the possible variability in the amplitude of the motions in the investigation. The results obtained from the 35 motion pairs, their mean and mean $\pm\sigma$ are presented in Figure 5.7. The curves given in the table indicate the % time the chosen part of the joint remains closed during the transient analysis. For example, if 5% of the area between the monoliths is taken as the spatial limit, that portion of the joint remains closed for 30%, 6% and 2% of the time for the gap values at 0.2cm, 1cm and 2cm's, respectively. If the motions are multiplied by 2, the ratio of the time the joints are closed increases. At 2x scale, a gap of 2cm's led to 5% of the joint between the monoliths closing for approximately 6% of the time of the ground motions on the mean curve. The curves obtained allowing for a greater area of the interface to be closed were naturally lower.

By selecting a reasonable limit on the ratio of area of the joint that may be closed, so that the joint behavior is not affected by pounding, one may reach a result on the required space that should be left between two monoliths to avoid coupled behavior between monoliths. For a limit as 10% of the area, it may be observed that at a scale of 2x and an opening value of 2cm, the ratio of the time the joint was closed reduced to around 10% on the mean plus one standard deviation curve. In other words, only 10% of the area between the monoliths was closed for a maximum of 10% of the time of the ground motions for 84% of the motions used. Therefore, it is very unlikely that monoliths with larger than 2cm spacing will go through pounding and coupling of the behavior that may affect the overall behavior of the system. Different valley widths and dam heights might yield different results, however results for dams with greater valley widths and shorter heights are expected to be on the safer side.

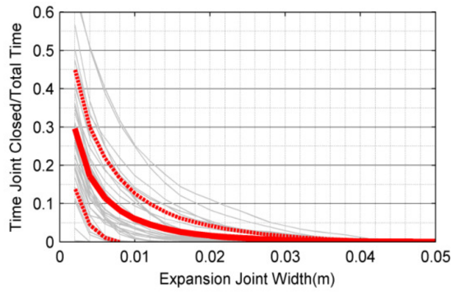

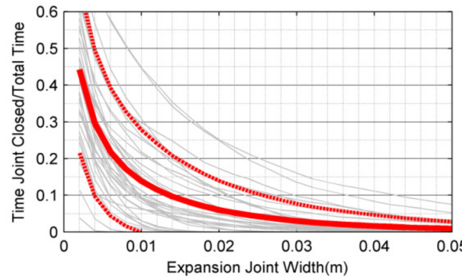

(a) 5% of the Interface Area for Scale=1 (b) 5% of the Interface Area for Scale=2

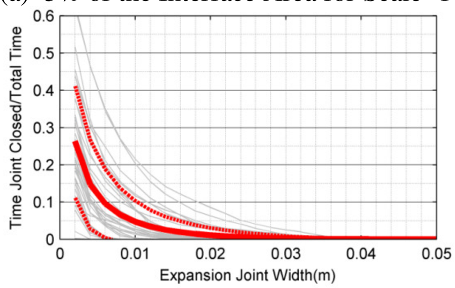

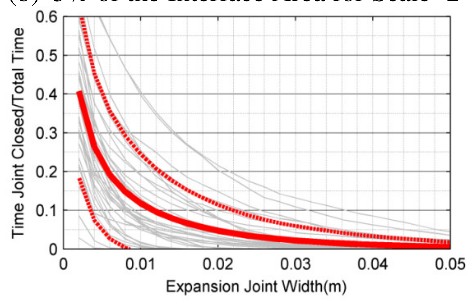

(c) 10% of the Interface Area for Scale=1 (d) 10% of the Interface Area for Scale=2

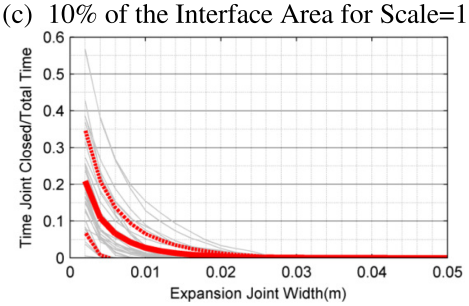

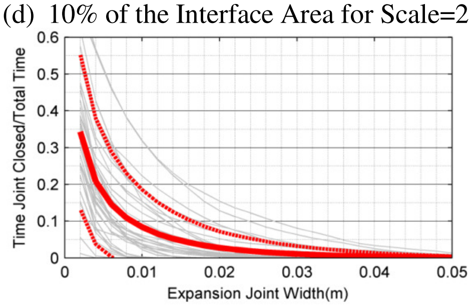

(e) 20% of the Interface Area for Scale=1 (f) 20% of the Interface Area for Scale=2

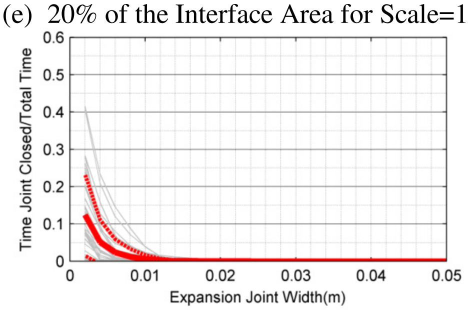

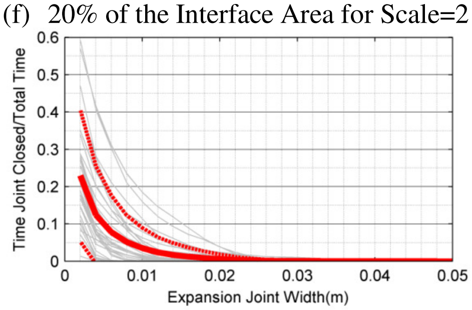

(g) 40% of the Interface Area for Scale=1 (h) 40% of the Interface Area for Scale=2

Figure 5.7 - Ratio of Time to the Total Duration that a Given Percentage of Joint Members are Closed for Different Joint Openings

5.4. EFFECT OF GROUND MOTION VARIABILITY

The bidirectional nature of the ground motions affects the behavior of a given system which is usually represented by the well-known 30% combination rule in the seismic design codes. In this section, an investigation of this effect for dam systems composed of monoliths was conducted. For a dam composed of monoliths, in which the monoliths affect each other, the quantification of this behavior is not very clear. Two different types of models were used in this study: first one included linear elastic interface elements between dam monoliths (signifying a transverse stiffness between the monoliths but no Coulomb Friction consideration) and the other including non-linear interface elements with Coulomb friction (low cohesion and low tanφ for this case) as described above.

Time history analyses were conducted in two different valley settings, with 240m and 480m valley widths, using various ground motion pairs, where each pair consisted of two ground motions with the fault-normal (FN) and the fault parallel (FP) components. For each pair two different analyses were conducted on each model with the FN record applied perpendicular to the dam axis and the FP record applied parallel, and the other vice versa. While each motion provided 3 records (fault normal, fault parallel and vertical) only the horizontal records were used in the study.

The ground motion pairs were obtained from the PEER Ground Motion Database This tool provides motions within specified parameters which are defined by the user. The motions were scaled according to the ASCE 7-10 provisions to fit the target spectrum in the range of 0.2T and 1.5T (T being the period of the first mode of vibration) which corresponded to 0.046 sec and 0.344 sec for the 240m model respectively and to 0.06 sec and 0.453 sec for the 480m model, respectively. The scaling was done such that the Mean Square Error (MSE) was minimum between the geometric mean of the two horizontal components of the ground motion record and the target spectrum within the range of target periods.

The Mean Square Error for each ground motion record is given by:

$$MSE = \frac{\sum_i w(T_i)\{\ln[SA^{target}(T_i)] - \ln[f * SA^{record}T_i]\}^2}{w(T_i)} \quad \textbf{(8)}$$

where;

T_i : The target periods

$w(T_i)$: The weigth applied for each period (for this case all $w(T_i)=1$)

SA^{target} and SA^{record}: The spectral acceleration values corresponding to the target period in the target spectrum and the spectrum of the ground motion record respectively

f: The scale factor of the ground motion record

In order to minimize MSE for the given record, the scale factor, f, is obtained by:

$$\ln f = \frac{\sum_i w(T_i) \ln\left(\frac{SA^{target}(T_i)}{SA^{record}(T_i)}\right)}{\sum_i w(T_i)} \quad \textbf{(9)}$$

Corresponding scale factor was then applied to their respective ground motion pairs. (A single factor was calculated for each pair.)

The input earthquake parameters presented in Table 5.3 were used to select 8 ground motion pairs for the 240m model and 6 pairs for the 480m model. The motion pairs and their respective scale factors and properties are presented in Table 5.4 and Table 5.5 for the models with 240m and 480m valley widths respectively. The resulting spectra, the mean and mean ±σ of the spectra are also shown in Figure 5.8 and Figure 5.9.

Table 5.3 – Input Parameters for Ground Motion Records

	Min	Max
Magnitude (M_w)	6.0	8.0
Fault Type	Strike-Slip	
R_{JB}	10 km	50 km
$R_{rupture}$	10 km	50 km
V_{s30}	500 m/s	3000 m/s

Table 5.4 - Properties of the Ground Motion Records Used for the 240 m Valley Width Model

Motion#	MSE	Scale Factor	Event	Year	Station	Magnitude	Mechanism	R_{jb}(km)	R_{rup}(km)	V_{s30}(m/s)
1	0,1017	1,4558	Parkfield	1966	Temblor pre-1969	6,19	Strike-Slip	16,00	16,00	527,9
2	0,0279	2,0841	Imperial Valley-06	1979	Cerro Prieto	6,53	Strike-Slip	15,20	15,20	659,6
3	0,0306	1,2595	Victoria, Mexico	1980	Cerro Prieto	6,33	Strike-Slip	13,80	14,40	659,6
4	0,0726	3,2063	Kocaeli, Turkey	1999	Arcelik	7,51	Strike-Slip	10,60	13,50	523,0
5	0,0813	1,6309	Hector Mine	1999	Hector	7,13	Strike-Slip	10,30	11,70	684,9
6	0,0914	2,8779	Chi-Chi, Taiwan-04	1999	CHY028	6,20	Strike-Slip	17,60	17,70	542,6
7	0,0979	3,6360	Chi-Chi, Taiwan-04	1999	CHY035	6,20	Strike-Slip	25,00	25,10	555,2
8	0,0564	3,7742	Chi-Chi, Taiwan-04	1999	CHY080	6,20	Strike-Slip	12,40	12,50	680,0

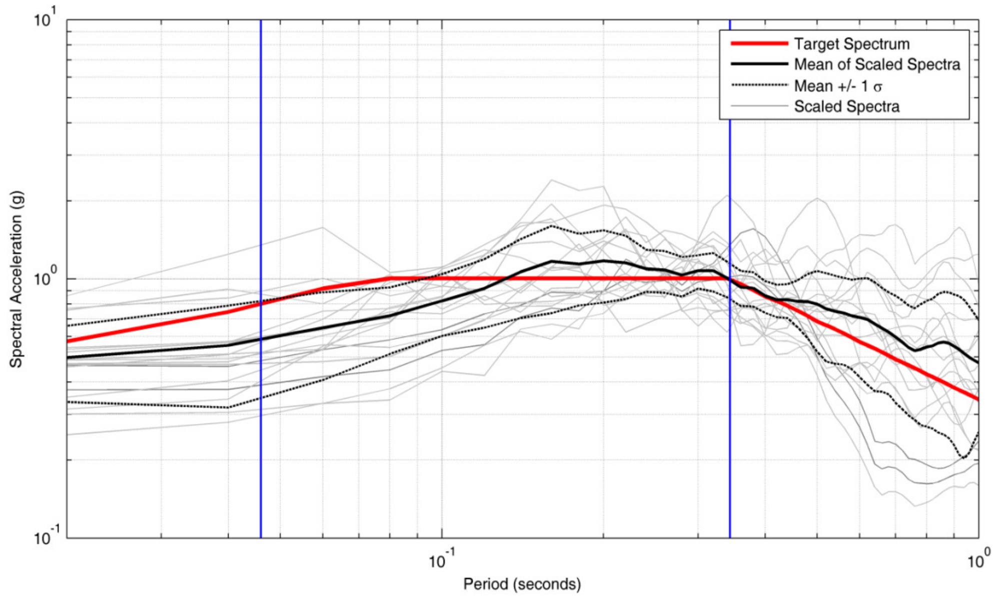

Figure 5.8 – Spectra of the Selected Ground Motions for the 240m Valley Width Model
(Blue Lines represent the target periods)

Table 5.5 - Properties of the Ground Motion Records Used for the 480 m Valley Width Model

Motion#	MSE	Scale Factor	Event	Year	Station	Magnitude	Mechanism	Rjb(km)	Rrup(km)	Vs30(m/s)
1	0,1017	1,5707	Parkfield	1966	Temblor pre-1969	6,19	Strike-Slip	16,00	16,00	527,9
2	0,0279	2,0687	Imperial Valley-06	1979	Cerro Prieto	6,53	Strike-Slip	15,20	15,20	659,6
3	0,0306	1,1523	Victoria, Mexico	1980	Cerro Prieto	6,33	Strike-Slip	13,80	14,40	659,6
4	0,0726	3,0244	Kocaeli, Turkey	1999	Arcelik	7,51	Strike-Slip	10,60	13,50	523,0
5	0,0813	1,3174	Hector Mine	1999	Hector	7,13	Strike-Slip	10,30	11,70	684,9
6	0,0914	2,9319	Chi-Chi, Taiwan-04	1999	CHY028	6,20	Strike-Slip	17,60	17,70	542,6

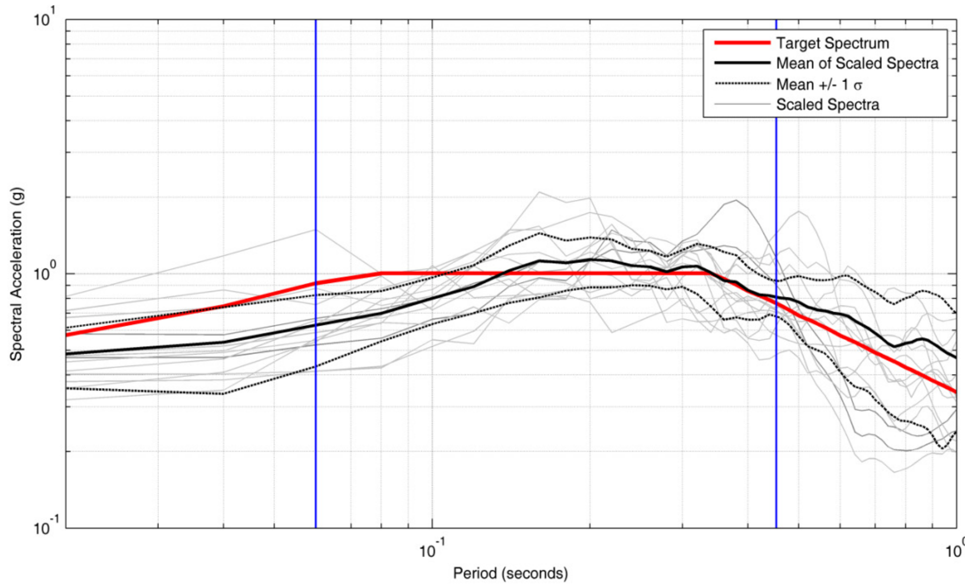

Figure 5.9 – Spectra of the Selected Ground Motions for the 480m Valley Width Model
(Blue Lines represent the target periods)

Maximum principal tensile stress values for the toe and heel areas of each monolith were selected as demand parameters for both the linear elastic and the coulomb friction model. The results given in Figure 5.10 and Figure 5.11 show that the two systems did not yield significantly different values in terms of principal tensile stress. The considered input motions did not create a significant non-linear behavior, i.e the transverse displacement joints between the monoliths tended to stay in the elastic range as given before in the 1 directional incremental dynamic analysis. The cross-valley motion did not seem to cause separation between the monoliths to lead to a meaningful change in the system behavior. However for the 240m model, the stress differences in the monoliths residing on the slopes were larger with respect to the monoliths in the center.

It should be noted that the principal tensile stress values in some cases far exceeded the tensile strength of the concrete. However since the objective of this study was to solely determine the effect of non-linearity in the expansion joints between the monoliths, a non-linear analysis involving cracking behavior was not implemented for the dam body.

Similar to the results presented in part 4.4 of this study the stresses in the heel areas were obtained with a large variance for a range of different ground motion records. As the records were scaled to fit a single target spectrum, this variation cannot be explained by the fundamental mode behavior assumption for the system. The frequency content of the input motion appears to significantly affect the stress at the toe. It was also observed that the stresses were both lower in average and showed small variation in the toe areas when compared to that of the heels.

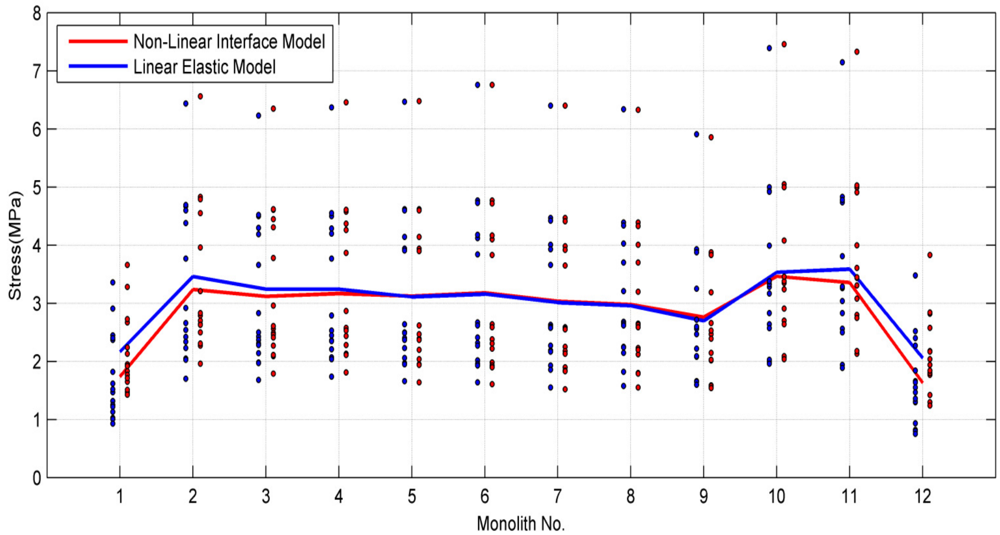

(a) Heels

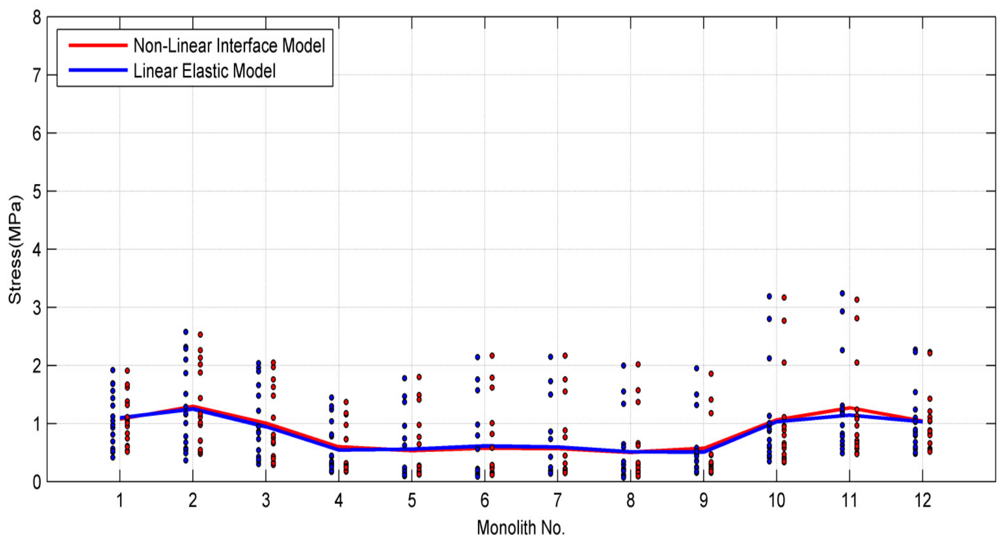

(b) Toes

Figure 5.10 - Maximum Principal Stress Values in Heels and Toes with Varying Ground Motion Pairs and Their Mean Curves, Valley Width= 240 m

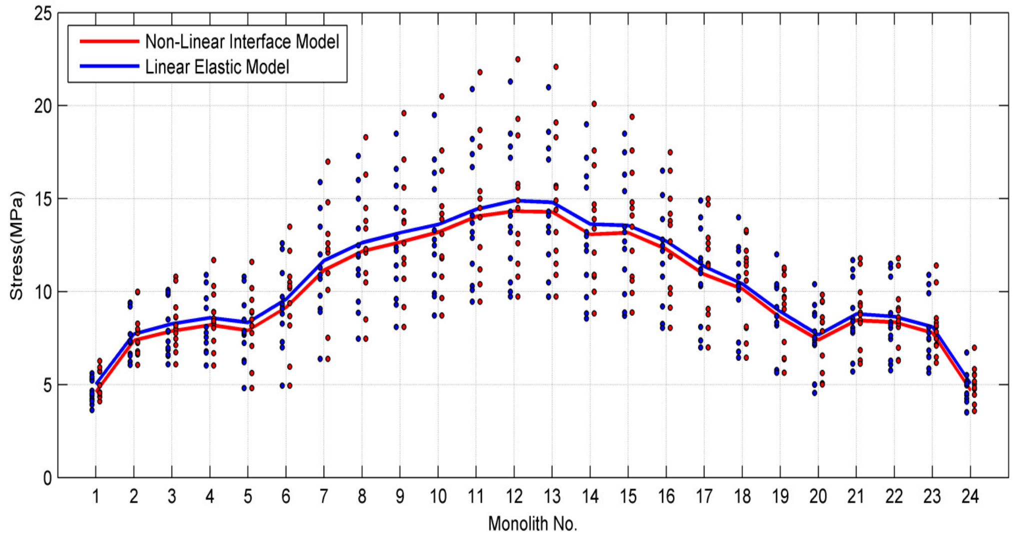

(a) Heels

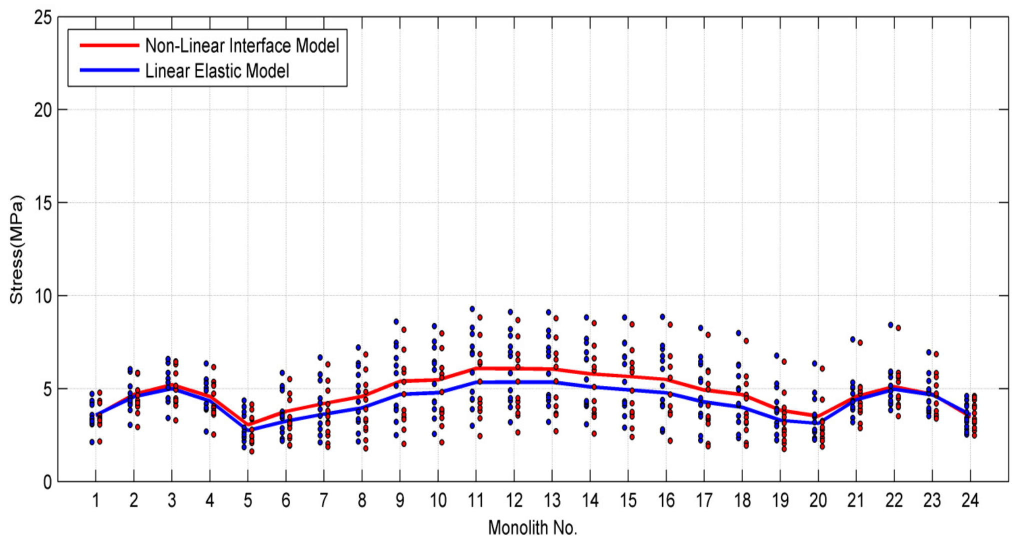

(b) Toes

Figure 5.11 - Maximum Principal Stress Values in Heels and Toes with Varying Ground Motion Pairs and Their Mean Curves, Valley Width= 480 m

CHAPTER 6

CONCLUSIONS AND OUTLOOK

6.1. CONCLUSIONS

The validity of the 2D modeling of concrete gravity dams was critically evaluated in this study using different sets of analyses. First, the frequency response functions for the 2D and 3D modeling idealizations of an 80m tall dam system were compared for 5 different valley widths. For the 3D models, 2 main types of idealized interface behavior was considered in this study, corresponding to a fully monolithic dam and a dam body comprised of completely independent monoliths connected only by the underlying foundation. The difference between the frequency and damping response was evaluated both among the 3D models as well as between the 2D and 3D models. As engineering demand parameters are time domain based parameters, a further comparison study was conducted to determine the difference in the response quantities in the time domain using the frequency response functions.

The evaluation of the effect of the interface behavior was treated next in the study. Instead of the idealized interface modeling as used above, different types of construction joints and the effect of the construction joint behavior on the system response was investigated using the transverse stiffness and Coulomb Friction parameters of the interface as design variables. The effect of motion in leading to sliding in the interface was evaluated in the US/DS direction using incremental dynamic analysis with these material models. Further on, the effect of bidirectional motion on the interface behavior (hence the system behavior) was considered using a set of bidirectional horizontal ground motions to evaluate the difference in some response parameters on the dam monoliths. The study also includes a critical evaluation of the construction joint width in order not to have closing of the interface between the monoliths using a set of bi-directional motions.

The following conclusions were obtained through the results of the study:

- The disparity between the effective damping factors of 3D models and the 2D SSI solution implied that the effective damping factor used in massless foundation models overestimated the damping in narrow valleys whereas it underestimated the damping for soft foundations.
- In general the 2D MF approach seemed to estimate the behavior of the 3D models with independent monoliths fairly using multiple ground motion records. For a fully monolithic system, even the use of multiple ground motions estimated the 3D solution poorly. Dams in narrow valleys have to be carefully evaluated in both the independent monolith and the fully monolithic settings.
- The results obtained in the study showed that the 2D approach, which is widely used in the analysis and design of concrete gravity dams, while yielding acceptable values when compared to 3D models in some cases, do not always yield accurate results. Even if the construction joints are built such that it creates no interaction between the monoliths, coupling due to the underlying foundation is evident.
- Even for the independent monolith systems with the largest V/H ratio and highest foundation stiffness, for which the disparity with the 2D solution is expected to be lowest, the individual results obtained from transient analyses of 3D systems yielded up to 100% difference when compared to the 2D solution. The selection of motions appears to be as important as the modeling approach for transient analyses.
- The coupling due to Soil-Structure Interaction is very effective in the response of these systems. Even in the widest valley setting (V/H=10) and using independent monoliths, the 2D model yielded a limited representation in both frequency and the time domain results.
- Contrary to the common intuition, the damping ratio did not seem to be a good indicator of demand parameters in the preliminary analysis stage. Although the damping ratios used in 3D MF and 2D MF models are similar, there was a great disparity in the transient analysis results between these models.

- For closing of the monolith interface, 10% of total joints being closed for 5% of the duration of motion was considered acceptable. The closing of the monoliths were found to be insignificant for joint openings larger than 2cm.
- The Coulomb Friction parameters used in the interface did not seem to affect the demand parameters of the system in an incremental dynamic analysis. The transverse stiffness of the interface was the dominating parameter in the response of these systems. The displacements of adjacent monolith were not high enough to create significant plastic deformations at the interface.

6.2. OUTLOOK

Some possible avenues for future research based on the findings in this study are:

- The damping correction for massless foundation models which are applied to estimate the soil-structure interaction should be reviewed for narrow valley widths. A further correction factor for V/H ratio could be the subject of future work.
- The results obtained from 3D massless models were compared to those obtained from both 2D massless foundation and 2D rigorous solution. These results could further be evaluated by comparing them to a 3D rigorous solution for assessing the overall accuracy of the massless model approach which has to be used in nonlinear transient analysis of dam systems.
- The non-linear behavior of the interface between monoliths could be further investigated using a wider range of interface properties, and ground motions.
- This study evaluated the representative value of 2D modeling when compared to 3D modeling. Further research can be conducted on how to improve the representative value for 2D models for preliminary analysis.

REFERENCES

1. Westergaard, H.M. (1933) Water Pressures on Dams during Earthquakes, Trans. ASCE, 98, 418–434.
2. Chopra, A.K. (1970). Earthquake Response of Concrete Gravity Dams, Journal of the Engineering Mechanics Division, 96(4), pp. 443-454.
3. Chopra, A.K. (1978). Earthquake Resistant Design of Concrete Gravity Dams, Journal of the Structural Division, 104(6), pp. 953-971.
4. Hall, J.F., Chopra, A.K. (1980). Dynamic response of embankment, concrete-gravity and arch dams including hydrodynamic interaction, Report No. UCB/EERC-80/39, Earthquake Engineering Research Center, University of California, Berkeley, Calif., 246 p.
5. Fenves, G., and Chopra, A. K. (1984). Earthquake Analysis and Response of Concrete Gravity Dams, Report No. UCB/EERC-84/10, Earthquake Engineering Research Center, University of California, Berkeley, Calif., 236 p.
6. Fenves, G., and Chopra, A. K. (1985). Simplified earthquake analysis of concrete gravity dams: Separate hydrodynamic and foundation interaction effects. Journal of engineering mechanics, 111(6), 715-735.
7. Fenves, G., and Chopra, A. K., (1986). Simplified Analysis for Earthquake Resistant Design of Concrete Gravity Dams, Report No. UCB/EERC-85/10, Earthquake Engineering Research Center, University of California, Berkeley, Calif., 144 p
8. Lotfi, V., Roesset, J.M., Tassoulas, J.L. (1987). A Technique for the Analysis of the Response of Dams to Earthquakes, Earthquake Engineering and Structural Dynamics, 15(4), pp. 463-490.
9. Medina, F., Dominguez, Tassoulas, JL. (1990). Response of Dams to Earthquakes Including Effects of Sediments, Journal of Structural Engineering, ASCE, 116(11), pp. 3108-3121.

10. Bougacha, S., Tassoulas, J.L. (1991). Seismic Analysis of Gravity Dams: 1. Modeling of Sediments, Journal of Engineering Mechanics, ASCE, 117(8), pp. 1826-1837.
11. Chopra, A.K., Zhang, L. (1991). Earthquake-Induced Base Sliding of Concrete Gravity Dams, Journal of Structural Engineering, ASCE, 117(12), pp 3698-3719.
12. Chávez, JW., Fenves, G. (1995). Earthquake Response of Concrete Gravity Dams Including Base Sliding, Journal of Structural Engineering, ASCE, 121(5), pp. 865-875.
13. Bhattacharjee S.S., Leger P., (1994). Application of NLFM Models to Predict Cracking in Concrete Gravity Dams, Journal of Structural Engineering-ASCE, 120(4), pp. 1255-1271.
14. Leger P; Leclerc (1996). Evaluation of earthquake ground motions to predict cracking response of gravity dams, Engineering Structures, 18(3), pp. 227-239.
15. Lysmer, J. and Kuhlemeyer, R.L. Finite dynamic model for infinite media Engineering Mechanics Division 1969.
16. Lysmer, J., Tabatabaie-Raissi, M., Tajirian, F., Vahdani, S., & Ostadan, F. (1983). SASSI. System for Analysis of Soil Structure Interaction, UC Berkeley, Dept. of Civil Engineering, Berkeley, CA.
17. U.S. Bureau of Reclamation (1976). Design of Gravity Dams, U.S. Government Printing Office, Denver, Colorado, 586 p.
18. United States Army Corps of Engineers (USACE) (1995). Seismic Design Provisions for Roller Compacted Concrete Dams, No. EP-1110-2-12.
19. Clough, R. W., Raphael, J. M., & Mojtahedi, S. (1973). ADAP-A computer program for static and dynamic analysis of arch dams. Berkeley, California: EERC 73-14.
20. Fenves, G., and Chopra, A. K., (1984). EAGD-84: A Computer Program for Earthquake Response Analysis of Concrete Gravity Dams, Report No. UCB/EERC-84/11, Earthquake Engineering Research Center, University of California, Berkeley, Calif., 102 p.

21. Fok, K., Hall, J.F., Chopra, A.K., (1986). EACD-3D: A Computer Program for Three-dimensional Earthquake Analysis of Concrete Dams, Report No. UCB/EERC-86/09, Earthquake Engineering Research Center, University of California, Berkeley, Calif., 159 p.
22. Tan, H., Chopra, A.K., (1996). EACD-3D-96: a computer program for three-dimensional earthquake analysis of concrete dams, UCB/SEMM-1996/06, Structural Engineering, Mechanics, Materials, University of California, Berkeley, Calif., 139 p
23. Wang, J., Chopra, A. K. (2008). EACD-3D-2008: A Computer Program for Three Dimensional Earthquake Analysis of Concrete Dams Considering Spatially-varying Ground Motion, Report No. UCB/EERC-2008/04, Earthquake Engineering Research Center, University of California, Berkeley, Calif., 151 p.
24. Domínguez, J., Maeso, O. (1993). Earthquake Analysis of Arch Dams. II: Dam-Water-Foundation Interaction, Journal of Engineering Mechanics, ASCE, 119(3), pp. 513-530.
25. Aznarez J.J., Maeso,O., Dominguez, J. (2006). BE analysis of bottom sediments in dynamic fluid-structure interaction problems, Engineering Analysis with Boundary Elements 30(2), pp. 124-136.
26. Lotfi V., Espandar, R., (2004). Seismic analysis of concrete arch dams by combined discrete crack and non-orthogonal smeared crack technique, Engineering Structures, 26(1), pp. 27-37.
27. Arabshahi H., Lotfi, V. (2008). Earthquake response of concrete gravity dams including dam-foundation interface nonlinearities, Engineering Structures, 30(11), pp. 3065-3073.
28. Rashed, A.A., Iwan, W.D. (1984). Hydrodynamic Pressure on Short-Length Gravity Dams Journal of Engineering Mechanics, ASCE, 110(9), September 1984, pp. 1264-1283.
29. U. Akpinar, A. Aldemir, B. Binici. (2011), Different Analysis Strategies For RCC Dam Desıgn. 5th International Conference on Advanced Computational Engineering and Experimenting (ACE-X2011), Algarve, 2011, Portugal.

30. Arici, Y., Binici, B., & Aldemir, A. (2014). Comparison of the expected damage patterns from two-and three-dimensional nonlinear dynamic analyses of a roller compacted concrete dam. Structure and Infrastructure Engineering, 10(3), 305-315
31. Chopra A.K. (2014). Earthquake analysis of concrete dams: factors to be considered. U.S. National Conference on Earthquake Engineering
32. Ghanaat, Y. (2004). Failure Modes Approach to Safety Evaluation of Dams, 13th World Conference on Earthquake Engineering, Vancouver, B.C., Canada.
33. Zhang, C., Jianwen, P., Jinting, W. (2009). Influence of seismic input mechanisms and radiation damping on arch dam response, Soil Dynamics and Earthquake Engineering, 29, 1282–1293.
34. Yücel, A.R. (2013) A user interface for seismic analysis of concrete gravity dams, M.Sc. Thesis, METU, Ankara.
35. Duygu, M.B (2014) Ground motion selection for the prediction of the Seismic response of concrete gravity dams, M.Sc. Thesis, METU, Ankara.
36. Erdoğan E.E. (2012) Investigation of the effect of soil structure interaction on the behavior of concrete faced rockfill dams and assesment of current analysis methodologies, M.Sc. Thesis, METU, Ankara
37. Kurama, Y. C., & Farrow, K. T. (2003). Ground motion scaling methods for different site conditions and structure characteristics. Earthquake engineering & structural dynamics, 32(15), 2425-2450.
38. O'Donnell, A. P., Kurama, Y. C., Kalkan, E., Taflanidis, A. A., & Beltsar, O. A. (2013). Ground motion scaling methods for linear-elastic structures: an integrated experimental and analytical investigation. Earthquake Engineering & Structural Dynamics, 42(9), 1281-1300.
39. O'Donnell, A. P., Beltsar, O. A., Kurama, Y. C., Kalkan, E., & Taflanidis, A. A. (2011). Evaluation of ground motion scaling methods for analysis of structural systems. ASCE Structures Congress.
40. Hong, Y.W., Du, C.B., Jiang, S.Y., (2011). Innovative Design and Construction of a High RCC Gravity Dam in High Seismic Intensity Region, Practice Periodical on Structural Design and Construction, 16(2), pp. 67-72.

APPENDIX A

EFFECTIVE DAMPING RATIOS AND RAYLEIGH DAMPING COEFFICIENTS FOR THE MF MODELS

f_1: Frequency of the first mode of vibration (Hz)

$\tilde{f}_1$: Frequency of the first mode of vibration for fixed base (Hz)

R_f, ε_1, ε_f, $\tilde{\varepsilon}_1$: The parameters used in (4)

α, β: Rayleigh Damping coefficients

Table A. 1 – Calculation of Effective Damping Ratios and Rayleigh Damping Coefficients for the MF Models

	Ef/Ec	f_1	$\tilde{f}_1$	R_f	ε_1	ε_f	$\tilde{\varepsilon}_1$	α	β
0x i	0.5	4.5976	5.4135	1.1774622	0.05	0.1300	0.161	5.55	0.0045
	1.0	4.9757	5.4135	1.0879876	0.05	0.0700	0.109	4.05	0.0028
	2.0	5.1843	5.4135	1.0442104	0.05	0.0350	0.079	2.95	0.0021
	4.0	5.2954	5.4135	1.0223024	0.05	0.0175	0.064	2.35	0.0017
0xm	0.5	6.0043	9.2276	1.5368319	0.05	0.1300	0.144	7.06	0.00275
	1.0	7.1463	9.2276	1.2912416	0.05	0.0700	0.093	5.20	0.00155
	2.0	8.0184	9.2276	1.1508032	0.05	0.0350	0.068	4.85	0.00080
	4.0	8.5746	9.2276	1.0761552	0.05	0.0175	0.058	4.35	0.00065
1x i	0.5	3.8359	5.4114	1.410725	0.05	0.1300	0.148	3.85	0.0056
	1.0	4.3580	5.4114	1.2417164	0.05	0.0700	0.096	2.80	0.0033
	2.0	4.8314	5.4114	1.120048	0.05	0.0350	0.071	2.40	0.0021
	4.0	5.0936	5.4114	1.062392	0.05	0.0175	0.059	2.05	0.0017
1xm	0.5	4.7032	7.1094	1.5116091	0.05	0.1300	0.144	5.30	0.0037
	1.0	5.5589	7.1094	1.2789221	0.05	0.0700	0.094	3.99	0.0021
	2.0	6.2072	7.1094	1.1453473	0.05	0.0350	0.068	3.60	0.0011
	4.0	6.6209	7.1094	1.0737815	0.05	0.0175	0.058	2.90	0.0011
2x i	0.5	3.5413	5.4052	1.5263321	0.05	0.1300	0.144	3.60	0.0057
	1.0	4.1757	5.4052	1.2944417	0.05	0.0700	0.093	2.60	0.0033
	2.0	4.6682	5.4052	1.1578767	0.05	0.0350	0.067	2.24	0.0021
	4.0	5.0022	5.4052	1.0805646	0.05	0.0175	0.057	2.10	0.0015
2xm	0.5	3.9879	6.1503	1.5422403	0.05	0.1300	0.144	4.28	0.0047
	1.0	4.7332	6.1503	1.2993958	0.05	0.0700	0.093	3.70	0.0021
	2.0	5.3116	6.1503	1.1578997	0.05	0.0350	0.067	2.92	0.0014
	4.0	5.6903	6.1503	1.0808393	0.05	0.0175	0.057	2.38	0.0013

Table A.1 (Continued)

	Ef/Ec	f_1	$\tilde{f}_1$	R_f	ε_1	ε_f	$\tilde{\varepsilon}_1$	α	β
4x i	0.5	3.3680	5.3954	1.6019596	0.05	0.1300	0.142	3.15	0.0064
	1.0	4.0430	5.3954	1.3345041	0.05	0.0700	0.091	2.50	0.0033
	2.0	4.5861	5.3954	1.176468	0.05	0.0350	0.066	2.08	0.0021
	4.0	4.9501	5.3954	1.0899578	0.05	0.0175	0.056	2.05	0.0015
4xm	0.5	3.5425	5.6908	1.6064361	0.05	0.1300	0.142	3.45	0.0058
	1.0	4.2548	5.6908	1.3375012	0.05	0.0700	0.091	2.85	0.0028
	2.0	4.8265	5.6908	1.1790739	0.05	0.0350	0.066	2.35	0.0018
	4.0	5.2115	5.6908	1.0919697	0.05	0.0175	0.056	2.05	0.0015
10x i	0.5	2.1625	2.6292	1.215815	0.05	0.1300	0.158	2.60	0.0090
	1.0	2.3887	2.6294	1.1007661	0.05	0.0700	0.107	2.05	0.0055
	2.0	2.5098	2.6295	1.047693	0.05	0.0350	0.078	1.40	0.0034
	4.0	2.5702	2.6296	1.023111	0.05	0.0175	0.064	1.30	0.0032
10xm	0.5	3.1488	5.3047	1.6846735	0.05	0.1300	0.140	2.40	0.0080
	1.0	3.9285	5.3068	1.3508464	0.05	0.0700	0.090	2.30	0.0035
	2.0	4.4742	5.3078	1.1863126	0.05	0.0350	0.065	1.65	0.0025
	4.0	4.8433	5.3084	1.0960296	0.05	0.0175	0.055	1.45	0.0020
2d	0.5	2.9168	5.1057	1.7504457	0.05	0.1300	0.139	3.60	0.00440
	1.0	3.5909	5.1057	1.4218441	0.05	0.0700	0.087	2.75	0.00230
	2.0	4.1640	5.1057	1.2261527	0.05	0.0350	0.062	2.26	0.00145
	4.0	4.5703	5.1057	1.1171477	0.05	0.0175	0.053	2.05	0.00120